**Akbar Ghazavizadeh**
Université Paris 13, LSPM-UPR3407 CNRS,
Sorbonne Paris Cité, avenue Jean-Baptiste
Clément, Villetaneuse 93430, France;
Arts et Métiers ParisTech, CNRS,
Université de Lorraine,
LEM3-UMR 7239 CNRS—4 rue Augustin
Fresnel, 57078 Metz, France;
Laboratoire Quartz,
Supméca, 3, rue Fernand Hainaut, 93407
St Ouen Cedex, France
e-mail: akbar.ghazavizadeh@univ-paris13.fr

**Fodil Meraghni**
Arts et Métiers ParisTech, CNRS,
Université de Lorraine,
LEM3-UMR 7239 CNRS—4 rue Augustin
Fresnel, 57078 Metz, France
e-mail: fodil.meraghni@ensam.eu

**Laurent Peltier**
Arts et Métiers ParisTech, CNRS,
Université de Lorraine,
LEM3-UMR 7239 CNRS—4 rue Augustin
Fresnel, 57078 Metz, France
e-mail: laurent.peltier@ensam.eu

**Nadine Bourgeois**
Arts et Métiers ParisTech, CNRS,
Université de Lorraine,
LEM3-UMR 7239 CNRS—4 rue Augustin
Fresnel, 57078 Metz, France
e-mail: nadine.bourgeois@univ-lorraine.fr

# A General Damage Accumulation Model for Multiaxial, Proportional High Cycle Fatigue Loadings With Sines, Crossland and Dang Van Criteria

*In this paper, a key differential equation is proposed to formulate fatigue damage evolution in metallic alloys under multiaxial, multiblock, proportional loadings in high cycle fatigue (HCF) and very high cycle fatigue (VHCF) regimes. This differential equation possesses two main components: one is a stress function to accommodate the adopted fatigue criterion and the other one is a characteristic damage function that serves to capture the HCF response of alloys. Two distinct characteristic damage functions with three different multiaxial fatigue criteria, namely Sines, Crossland, and Dang Van criteria, are examined to develop six (out of many possible) variants of the presented damage accumulation model. As a validation measure, Chaboche's HCF damage model is retrieved as a specific case of the developed formalism. For model parameters identification, an ad hoc two-level identification scheme is designed and numerically verified. It is demonstrated that endurance limit, which is determined from fully reversed HCF tests (i.e., $R=-1$), can be identified from fatigue tests with positive stress ratio ($R>0$), thus making our development quite suitable for specimens prone to buckling under compression. Another salient feature of the devised identification scheme is its capability in extracting model parameters from noisy data.* [DOI: 10.1115/1.4044455]

*Keywords: HCF/VHCF in metallic alloys, cumulative fatigue damage, multiaxial multiblock proportional loading, multiaxial fatigue criteria, parameters identification*

## 1 Introduction

High cycle fatigue (HCF) and very high cycle fatigue (VHCF) loading conditions are ubiquitous in mechanical systems ranging from household appliances to transportation vehicles. Because failure due to HCF and VHCF usually takes place without any prior warning that may lead to another catastrophic failure on a larger scale, there has been a growing interest in understanding and modeling this phenomenon.

Since Wöhler's monumental work on studying the fatigue life of railway axles [1], quite a few researchers have tried to investigate this failure mode in further details. Basquin [2] was the first who represented the tabulated data gathered by Wöhler in logarithmic scale to obtain the so-called S–N curve. He also proposed a power-law equation to approximate the S–N curve. An S–N curve serves to find the number of cycles to failure corresponding to a given stress amplitude in a fully reversed tension-compression (zero mean stress) loading. In most practical cases, however, the mechanical element undergoes time varying, multiaxial stresses during their service life. Such issues add to the complexity of fatigue life assessment and a sole S–N curve is not sufficient. Strictly speaking, for fatigue loadings where the stress amplitude is nonuniform and/or the mean stress is nonzero, one needs an appropriate fatigue damage accumulation rule as well as a suitable fatigue criterion for life estimation purposes.

The first and simplest cumulative fatigue damage theory, which is more or less widely used in the industry, is Palmgren–Miner's rule proposed independently by Palmgren [3] and Miner [4]. This simplistic model implies a linear summation of life fractions for a multiblock loading case. As its major drawbacks, this linear damage rule fails to incorporate the load sequence effects, load level dependence, and nonlinearity of damage evolution. Later on, Marco and Starkey [5] modified Palmgren–Miner's rule by adding a load-dependent exponent to the fraction expression. However, they did not specify the proper functional form for the exponent of their model. Besides, the critical damage value is a function of the load sequence unless the equivalent number of cycles method proposed in Ref. [6] is employed. Moreover, their damage model does not take into account the damage due to loadings below the endurance limit. Despite the improvements on Palmgren–Miner's rule, Marco and Starkey's rule did not gain the popularity of its predecessor.

Numerous other improvements and modifications to Palmgren–Miner's rule have subsequently been published. A fairly comprehensive literature review of the proposed cumulative fatigue damage models was undertaken by Fatemi and Yang [7]. Most of such models, however, fail to respond to the damage due to multiaxial, nonuniform, low-amplitude fatigue loadings. The fatigue damage accumulation models (DAMs) that are investigated in this study belong to continuum damage mechanics (CDM) models. The basic idea of CDM models lies in following the evolution of a dimensionless, continuous scalar that represents the damage. As one of their advantages, CDM models enable incorporation of damage due to other mechanisms such as creep. The interested reader can consult Refs. [8–12], among others, for an exhaustive discussion.

The success of continuum damage theories elaborated by Rabotnov [13,14] and Kachanov [15] for explaining the damage

in materials subjected to creep [16,17] was the motivating factor in extending the idea to fatigue damage. One of the first and most famous fatigue accumulation models developed in the context of CDM is Chaboche's fatigue DAM [18,19], which was first presented for simple uniaxial loadings [18] followed by more general versions of the model presented later on Refs. [20,21]. In light of the success of Chaboche's DAM, we develop in the current investigation a more general framework in the context of CDM from which Chaboche's DAM is retrieved as a specific case. The new development is predicated on a damage rate equation proposed by Lemaitre [10] for *brittle damage*. A damage is called brittle when cracks are initiated at the mesoscale without a large amount of plastic strain. Because no large-scale plasticity is involved in HCF and VHCF regimes, one can safely assume that HCF and VHCF failure can be described by means of the brittle damage mechanism, as exploited in Refs. [22–24], to mention but a few. To demonstrate the versatility of the presented formalism, six different variants of our proposed DAM are developed and numerically implemented using two characteristic damage functions and three popular multiaxial fatigue criteria.

Fatigue criteria are purported to modify the endurance limit (also known as the fatigue strength) as a function of the deviation from zero mean stress. By definition, the endurance limit is the threshold of the stress amplitude in a fully reversed, uniaxial, fatigue test below which the fatigue failure does not take place. Early empirical fatigue criteria for uniaxial loading were proposed by Gerber [25], Goodman [26], Haigh [27], and Soderberg [28]. For multiaxial loading, however, more sophisticated criteria are required. In-depth discussions and critical comparisons of a large number of available criteria can be found, among other studies, in Refs. [29–33]. The multiaxial fatigue criteria that are adopted in this study are Sines [34], Crossland [35], and Dang Van criteria [36,37]. Carpinteri and co-authors argue that for practical engineering applications under multiaxial proportional loading, Sines and Crossland criteria have been successful [38]. These two criteria belong to the class of stress-invariant multiaxial fatigue criteria. The third multiaxial criterion that is employed in this work is the Dang Van criterion, which belongs to the critical plane approaches. This criterion was indeed devised to address the insufficiencies of other criteria under nonproportional loading. This notwithstanding, it is specialized in proportional loading applications for the purposes of the current study.

The underlying assumptions of the present analysis are summarized here. In addition to the proportionality of loading and nonexistence of any visible crack, it is assumed that there are no plastic deformations involved in the fatigue loading. It is additionally assumed that the damage is isotropic and can be represented by means of a single scalar variable $D$. For the applications of this study, the end of the fatigue life is equivalent to the crack initiation stage. The growth of the cracks that are created due to HCF or VHCF loadings, as the last stage of the fatigue failure, is not the subject of this study and microdefects closure effects are ignored. Moreover, DAM variants that are developed in this study are primarily isothermal and no temperature variable appears in their mathematical representation. Finally, the impact of cycling frequency is neglected in the (V)HCF response of materials describable by the models studied here.

To give a concrete example of the potential applications of the methodology of this work, consider fatigue test specimens cut from thin aluminum sheets. Mechanically, such specimens have a negligible resistance to buckling, which precludes fatigue tests with negative stress ratio. Consequently, the fatigue endurance limit of these specimens cannot be measured from fully reversed HCF tests. Using the identification procedure elaborated in Sec. 3, this material property together with parameters of the adopted DAM variant can be identified from HCF tests with positive stress ratio performed on these specimens. The identification results can then be plugged into the adopted DAM variant to estimate the fatigue life of 3D structural members made of the initial aluminum sheets and subjected to multiaxial proportional cyclic loadings.

To briefly enumerate the highlights of the present investigation, a key differential equation is developed in the context of continuum damage mechanics to follow the evolution of isotropic damage in metallic alloys. Our proposed (V)HCF-DAM (damage accumulation model for HCF and VHCF regimes) is a nonlinear model primarily developed for multiaxial, proportional, cyclic loadings, capable of taking into account the effect of damage history, nonzero hydrostatic stress, and low-amplitude cycles. To illustrate the performance of our methodology, six different variants of our DAM are developed using three popular multiaxial fatigue criteria of Sines, Crossland, and Dang Van. Chaboche's cumulative fatigue damage equation for 3D loading is recovered as a specific DAM variant of this work, thus corroborating the underlying assumptions and the key differential equation. Additionally, we propose an efficient identification procedure that is capable of identifying the model parameters and also the endurance limit of alloys, quite satisfactorily from noisy fatigue data. In addition to being noisy, all fatigue data are characterized by $R>0$, which is appropriate for specimens susceptible to buckling under compression. These features underline the robustness and the efficacy of the proposed identification scheme.

The rest of this contribution is organized as follows: we begin with the kinetic damage evolution law of Lemaitre and make use of the above-mentioned assumptions to obtain the key differential equation of this work, Eq. (10), expressed in terms of cycles differential and loading characteristics for multiaxial proportional loadings. This key equation possesses two principal degrees of freedom that make it general enough to not only recover the well-known Chaboche's DAM but also to develop one's own customized analytical forms. One of the degrees of freedom is directly related to the adopted fatigue criterion. Prior to the application of each fatigue criterion, the key differential equation has to be adapted accordingly. In order to make this equation compatible with Sines and Crossland criteria, it needs to be expressed in terms of octahedral shear stress amplitude. The necessary mathematical details allowing for this adaptation are provided in Appendix A. Application of Dang Van criterion in conjunction with the key equation requires a different adaptation, which is elaborated in Appendix B. The other degree of freedom of the principal equation concerns some characteristic damage function that is more or less subjective and highly depends on the user's level of expertise. Two distinct characteristic damage functions from the literature are examined, which in combination with three above-mentioned fatigue criteria, lead to six analytical, closed-form DAM variants of the present investigation. These variants are six examples of countless analytical DAMs that are obtainable from countless combinations of fatigue criteria and characteristic damage functions. Section 3 gives the details of the best practice to identify the model parameters of DAM variants developed in this study using their reduced form of uniaxial loading. Therein, it is explained how to identify the fatigue endurance limit of metallic alloys from tension–tension fatigue tests (i.e., $R>0$). This is the case of test specimens susceptible to buckling under compression. The efficiency and robustness of the delineated identification procedure to noisy data are also assessed. Section 4 is dedicated to the discussion and generalization of the proposed approach. Concluding remarks and the significant findings of the investigation are given in Sec. 5.

## 2 Development of the High Cycle Fatigue Damage Accumulation Model for Multiaxial, Multiblock, Proportional Loadings

The CDM driven model of HCF damage accumulation that is developed hereunder is founded on a damage rate equation derived by Lemaitre for brittle damage [39–41]. Brittle damage is characterized by the creation of defects without measurable macroscopic plastic strain. Lemaitre [41] asserts that high cycle fatigue of metals is one of the cases in which plastic strain may be reasonably neglected. As such, one can safely assume that HCF and VHCF

failures can be described by the brittle damage mechanism. This general idea has widely been exploited in Refs. [22–24] among others, to model HCF response of the alloys investigated. However, the majority of these models are limited to the simple case of uniaxial fatigue loading with simple uniaxial fatigue criteria, such as Goodman's criterion, in contrast with the more general and more versatile (V)HCF-DAM of this study, as demonstrated in the following.

The (V)HCF-DAM that is proposed here is developed from the following rate equation derived in Ref. [10] and exploited by Refs. [22–24], among many others.

$$\dot{D} = BY^{\frac{\theta}{2}-1}\dot{Y} \tag{1}$$

In the above evolution equation, $\theta$ is a material parameter and

$$Y = \frac{{\sigma_{\mathrm{eq}}}^2}{2E_0(1-D)^2} f(\sigma_{\mathrm{H}}/\sigma_{\mathrm{eq}}) \tag{2}$$

$\sigma_{\mathrm{H}} = \sigma_{kk}/3$ is the hydrostatic stress and $\sigma_{\mathrm{eq}}$ is expressed as follows in terms of deviatoric stress.

$$\sigma_{\mathrm{eq}} = \left(\frac{3}{2}\mathbf{S}_{ij}\mathbf{S}_{ij}\right)^{0.5}, \quad \mathbf{S}_{ij} = \boldsymbol{\sigma}_{ij} - \sigma_{\mathrm{H}}\boldsymbol{\delta}_{ij} \tag{3}$$

Function $f$, on the other hand, has the following representation

$$f(\sigma_{\mathrm{H}}/\sigma_{\mathrm{eq}}) = \frac{2}{3}(1+\upsilon) + 3(1-2\upsilon)(\sigma_{\mathrm{H}}/\sigma_{\mathrm{eq}})^2 \tag{4}$$

As explained in Ref. [42], for isothermal high cycle fatigue, $B = B(D, \boldsymbol{\sigma})$ is a function of the stress state and damage variable. The way the mathematical form of $B$ is determined is elaborated further below. Under proportional loading conditions, it can be demonstrated that [22,42]

$$\dot{D} = \frac{\bar{B}\sigma_{\mathrm{eq}}^{\theta-1}\dot{\sigma}_{\mathrm{eq}}}{(1-D)^{\theta}} \quad \text{where} \quad \bar{B} = 2^{1-\frac{\theta}{2}} B f^{\frac{\theta}{2}}(\sigma_{\mathrm{H}}/\sigma_{\mathrm{eq}}) E_0^{-\frac{\theta}{2}} \tag{5}$$

Moreover, under proportional loading, $f^{\theta/2}(\sigma_{\mathrm{H}}/\sigma_{\mathrm{eq}}) = \text{constant}$ [22,42]. Naturally, $\dot{D} > 0$ when $\dot{\sigma}_{\mathrm{eq}} > 0$ and $\dot{D} = 0$ if $\dot{\sigma}_{\mathrm{eq}} \leq 0$, simply because negative damage rate is not physical.

The above damage evolution equation is expressed in time differential form, which makes it less suitable for practical applications. The time differential equation (5) is therefore integrated over one cycle in order to eliminate the time differential in favor of the differential of cycles. Since the differential of von Mises equivalent stress appears on the right-hand side, the variation of this variable over one cycle is required. Assuming that the loading is proportional and given that von Mises equivalent stress is always positive, four distinct states may arise for the diagram of $\sigma_{\mathrm{eq}}$ with respect to $\gamma(t)$, the time coefficient of the proportional stress tensor, as demonstrated in Fig. 1. Here, $\gamma_m = \min(\gamma)$ and $\gamma_{\mathrm{M}} = \max(\gamma)$. By definition, the time-varying, proportional stress tensor $\boldsymbol{\sigma}(t, \boldsymbol{X})$ at the point $\boldsymbol{X}$ can be decomposed as follows where $\gamma$ is the time-varying proportionality coefficient and stress tensor $\boldsymbol{\Sigma}$ is independent of time.

$$\boldsymbol{\sigma}(t, \boldsymbol{X}) = \gamma(t)\boldsymbol{\Sigma}(\boldsymbol{X}) \tag{6}$$

Considering the above illustration, the time differential Eq. (5) is integrated over $\Omega$, the domain of one complete cycle of loading. Without loss of generality, we assume that the extremes of $\Omega$, respectively, coincide the start and end of the ascending and descending paths of a period in $\gamma(t)$.

$$\frac{\mathrm{d}D}{\mathrm{d}N} = \int_{\Omega} \dot{D}\mathrm{d}t = \int_{\Omega} \frac{\bar{B}\sigma_{\mathrm{eq}}^{\theta-1}\dot{\sigma}_{\mathrm{eq}}}{(1-D)^{\theta}}\mathrm{d}t = \int_{\Omega} \frac{\bar{B}\sigma_{\mathrm{eq}}^{\theta-1}}{(1-D)^{\theta}}\mathrm{d}\sigma_{\mathrm{eq}} \tag{7}$$

With regard to cases (a) and (b) of Fig. 1, there is one ascending path within $\Omega$ where $\dot{\sigma}_{\mathrm{eq}} > 0$. For these two cases, the change in the damage variable per cycle is readily obtained by calculating the integral (7) over the respective ascending path.

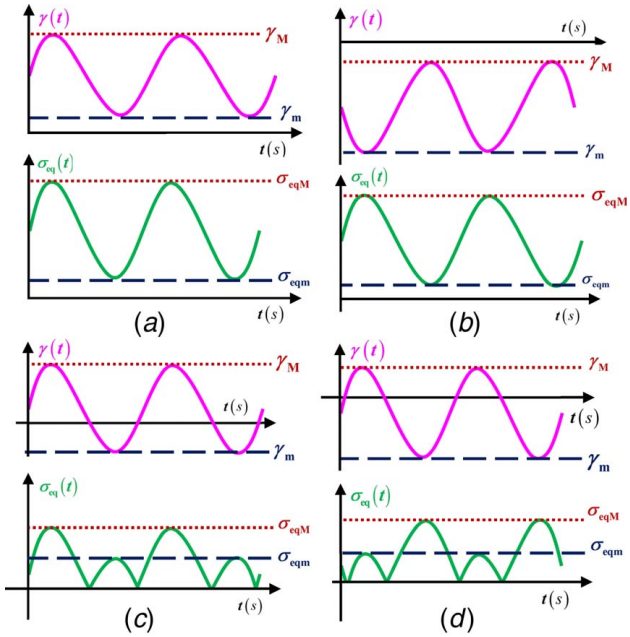


**Fig. 1 Schematic representation of four distinct possible cases that may occur for $\gamma(t)$ and its impact on $\sigma_{\mathrm{eq}}$: (a) $\gamma_{\mathrm{m}} > 0$; (b) $\gamma_{\mathrm{M}} < 0$; (c) $\gamma_{\mathrm{m}}\gamma_{\mathrm{M}} < 0$ and $|\gamma_{\mathrm{M}}| > |\gamma_{\mathrm{m}}|$; and (d) $\gamma_{\mathrm{m}}\gamma_{\mathrm{M}} < 0$ and $|\gamma_{\mathrm{M}}| < |\gamma_{\mathrm{m}}|$**

$$\frac{\mathrm{d}D}{\mathrm{d}N} = \int_{\sigma_{\mathrm{eq_m}}}^{\sigma_{\mathrm{eq_M}}} \frac{\bar{B}\sigma_{\mathrm{eq}}^{\theta-1}}{(1-D)^{\theta}}\mathrm{d}\sigma_{\mathrm{eq}} = \frac{2\bar{B}}{\theta(1-D)^{\theta}}(\sigma_{\mathrm{eq_M}}^{\theta} - \sigma_{\mathrm{eq_m}}^{\theta}) \tag{8}$$

For cases (c) and (d) of Fig. 1, there are two ascending paths within $\Omega$ where $\dot{\sigma}_{\mathrm{eq}} > 0$. For these two cases, the change in the damage variable per cycle is obtained by breaking the integral over two intervals within which the integrand is nonzero.

$$\begin{aligned}\frac{\mathrm{d}D}{\mathrm{d}N} &= \int_{0}^{\sigma_{\mathrm{eq_m}}} \frac{\bar{B}\sigma_{\mathrm{eq}}^{\theta-1}}{(1-D)^{\theta}}\mathrm{d}\sigma_{\mathrm{eq}} + \int_{0}^{\sigma_{\mathrm{eq_M}}} \frac{\bar{B}\sigma_{\mathrm{eq}}^{\theta-1}}{(1-D)^{\theta}}\mathrm{d}\sigma_{\mathrm{eq}} \\ &= \frac{2\bar{B}}{\theta(1-D)^{\theta}}(\sigma_{\mathrm{eq_M}}^{\theta} + \sigma_{\mathrm{eq_m}}^{\theta})\end{aligned} \tag{9}$$

To calculate the two previous integrals, it is assumed that the damage variable does not change over the domain of one cycle [22,42]. The last two differential equations can be unified into a single equation as below

$$\frac{\mathrm{d}D}{\mathrm{d}N} = \frac{2\bar{B}}{\theta(1-D)^{\theta}}[\sigma_{\mathrm{eq_M}}^{\theta} - \mathrm{sign}(R_{\mathrm{p}})\sigma_{\mathrm{eq_m}}^{\theta}] \tag{10}$$

where the proportionality ratio $R_{\mathrm{p}} = \gamma_m/\gamma_{\mathrm{M}} = \sigma_{ij_{\mathrm{m}}}/\sigma_{ij_{\mathrm{M}}}$. With this definition for $R_{\mathrm{p}}$, its variation is confined to $-\infty < R_{\mathrm{p}} < 1$, in analogy with the stress ratio $R = \sigma_{\mathrm{m}}/\sigma_{\mathrm{M}}$, used for uniaxial cyclic loadings. In light of the development of Appendix A, Eq. (10) is recast as a function of $A_{\mathrm{II}}$, the octahedral shear stress amplitude for proportional loading (see e.g., Eq. (9) in Ref. [21]).

$$\frac{\mathrm{d}D}{\mathrm{d}N} = \frac{2^{\theta+1}\bar{B}{A_{\mathrm{II}}}^{\theta}}{\theta(1-D)^{\theta}} \frac{1 - \mathrm{sign}(R_{\mathrm{p}})[|R_{\mathrm{p}}|^{\mathrm{sign}(R_{\mathrm{p}}+1)}]^{\theta}}{[1 - \mathrm{sign}(R_{\mathrm{p}})|R_{\mathrm{p}}|^{\mathrm{sign}(R_{\mathrm{p}}+1)}]^{\theta}} \tag{11}$$

where $A_{\mathrm{II}} = \frac{1}{2}\sqrt{\frac{3}{2}[(S_{1\mathrm{M}} - S_{1\mathrm{m}})^2 + (S_{2\mathrm{M}} - S_{2\mathrm{m}})^2 + (S_{3\mathrm{M}} - S_{3\mathrm{m}})^2]}$.

$A_{\mathrm{II}}$ is frequently utilized in works on multiaxial fatigue loadings; hence, the new representation of the key differential equation of

damage evolution. The above differential equation serves as the basis for the subsequent DAM relations with Sines or Crossland criteria. In reference to Eq. (5) and knowing that $B = B(D, \boldsymbol{\sigma})$, $\bar{B}$ is a function of $D$ and $\boldsymbol{\sigma}$, at a constant temperature. To proceed with the damage model development, a substantial assumption is made here that $\bar{B}$ can be multiplicatively decomposed as follows

$$\bar{B}(D, \boldsymbol{\sigma}) = H(D)M(\boldsymbol{\sigma}) \tag{12}$$

where $H$ and $M$ are, respectively, scalar functions of the damage variable and the stress tensor. Substitution of the above decomposition into the differential equation (11) leads to

$$\frac{(1-D)^{\theta}\mathrm{d}D}{H(D)} = 2^{\theta+1}{A_{\mathrm{II}}}^{\theta}\frac{M(\boldsymbol{\sigma})}{\theta}\frac{1-\mathrm{sign}(R_{\mathrm{p}})[|R_{\mathrm{p}}|^{\mathrm{sign}(R_{\mathrm{p}}+1)}]^{\theta}}{[1-\mathrm{sign}(R_{\mathrm{p}})|R_{\mathrm{p}}|^{\mathrm{sign}(R_{\mathrm{p}}+1)}]^{\theta}}\mathrm{d}N \tag{13}$$

The central idea of the remaining procedure lies in choosing a proper mathematical form for $H(D)$, referred to as characteristic damage function, in the first place. The functional form of $M(\boldsymbol{\sigma})$ will subsequently be determined from the adopted multiaxial fatigue criterion. Once this criterion is known, $M(\boldsymbol{\sigma})$ is calculated by studying two specific limit cases of identical fatigue lives and equating them, as elaborated in the following. Listed below are two different functions of $H(D)$ that are examined in this work, as they are usually adopted in the relevant literature [43] and [19,44], respectively.

$$\text{(i). } H(D) = (1-D)^{\theta}D^{\alpha} \quad \text{(ii). } H(D) = [1-(1-D)^{1+\theta}]^{\alpha}$$

For each case of $H(D)$, three multiaxial fatigue criteria, namely Sines, Crossland, and Dang Van, summarized below, are studied to find their associated $M(\boldsymbol{\sigma})$, thereby determining the damage evolution laws for a generic cyclic loading block.

$$\text{Sines: } A_{\mathrm{II}} - A^{*}_{\mathrm{Sns}} \le 0, \quad A^{*}_{\mathrm{Sns}} = \sigma_{1_0}(1-3b\bar{\sigma}_{\mathrm{H}})$$

$$\text{Crossland: } A_{\mathrm{II}} - A^{*}_{\mathrm{CL}} \le 0, \quad A^{*}_{\mathrm{CL}} = \sigma_{1_0}\frac{1-3b\sigma_{\mathrm{H_M}}}{1-b\sigma_{1_0}}$$

$$\text{Dang-Van: } \tau_{\mathrm{a}} - A^{*}_{\mathrm{DV}} \le 0, \quad A^{*}_{\mathrm{DV}} = \sigma_{1_0}\frac{1-3b\sigma_{\mathrm{H_M}}}{2(1-b\sigma_{1_0})}$$

Application of Dang Van criterion requires a different differential equation than Eq. (13). Appendix B is devoted to the derivation of Eq. (B13), which is the analogue of Eq. (13) and is specifically developed for using Dang Van criterion with the damage accumulation model of this work. Therefore, different forms of $H(D)$ and different multiaxial fatigue criteria give rise to different variants of DAM. As such, each variant is characterized by the functional form chosen for $H$ and the adopted fatigue criterion. For example, Crossland-$H_{(\mathrm{i})}$ denotes the variant of damage model (13) in which $H$ of case (i) is employed for the integral operation, and Crossland fatigue criterion is used for determining $M(\boldsymbol{\sigma})$, thus completing the explicit expression of the DAM variant.

**2.1 Case (i): $\boldsymbol{H(D) = (1-D)^{\theta}D^{\alpha}}$.** This first choice for $H(D)$ helps to cancel the term $(1-D)^{\theta}$ on the left-hand side of the differential equation (13) and leaves the remaining expression explicitly integrable. With this particular choice, the resulting differential equation looks like the evolution law $\dot{D} = \varphi D^{\zeta}$, which has been exploited by Patil et al. [43], where φ and $\zeta$ are two unknown functions of the loading state. They argue that the above form leads to good results for the problems they had studied. For the exponent $\alpha$, Dattoma et al. [45] proposed a slight modification to the form suggested by Chaboche [19] and Lesne and Chaboche [44]. Their modified form of $\alpha$ function, given in Eq. (14), is adopted in the present study. Knowing that $\alpha$ is a function of the adopted fatigue criterion, for different fatigue criteria examined in this study, the corresponding $\alpha$ functions are given below.

$$\alpha_{\mathrm{Sns}} = 1 - a\left(\frac{\langle A_{\mathrm{II}} - A^{*}_{\mathrm{Sns}}\rangle}{\sigma_{\mathrm{u}} - \sigma_{\mathrm{eq_M}}}\right)^{\zeta}, \quad \alpha_{\mathrm{CL}} = 1 - a\left(\frac{\langle A_{\mathrm{II}} - A^{*}_{\mathrm{CL}}\rangle}{\sigma_{\mathrm{u}} - \sigma_{\mathrm{eq_M}}}\right)^{\zeta},$$

$$\alpha_{\mathrm{DV}} = 1 - a\left(\frac{\langle \tau_{\mathrm{a}} - A^{*}_{\mathrm{DV}}\rangle}{\sigma_{\mathrm{u}} - \sigma_{\mathrm{eq_M}}}\right)^{\zeta} \tag{14}$$

In above $\alpha$ functions, $\zeta$ and $a$ are the model parameters. In fact, $\alpha$ function of Chaboche's damage model lacks exponent $\zeta$ of the expression between parentheses. With this proposed form for $H(D)$, the solution to the governing differential equation (13) is readily obtained by examining two numerical possibilities for $\alpha$ exponent, namely $0 < \alpha < 1$ and $\alpha = 1$, because of Macaulay brackets operator. The former is related to the HCF region and the latter to VHCF region. In what follows, we first employ Sines and Crossland criteria to obtain the corresponding damage evolution laws, as their solutions are closely linked. Then, the damage evolution expression with $H_{(\mathrm{i})}$ and Dang Van criterion is presented.

*2.1.1 Sines-$\mathrm{H}_{(i)}$ Variant—High Cycle Fatigue Part ($0 < \alpha < 1$).* Since the HCF regime of loading is concerned, $0 < \alpha < 1$. Substituting $H_{(\mathrm{i})}$ into Eq. (13) gives

$$\int_{D_{i-1}}^{D_i}\frac{\mathrm{d}D}{D^{\alpha}} = \int_0^{N_i}\frac{M(\boldsymbol{\sigma}_i)}{\theta}\frac{2^{\theta+1}[1-\mathrm{sign}(R_{\mathrm{p}})[|R_{\mathrm{p}}|^{\mathrm{sign}(R_{\mathrm{p}}+1)}]^{\theta}]_i}{{A_{\mathrm{II}_i}}^{-\theta}[1-\mathrm{sign}(R_{\mathrm{p}})|R_{\mathrm{p}}|^{\mathrm{sign}(R_{\mathrm{p}}+1)}]_i^{\theta}}\mathrm{d}N$$

$$\Rightarrow \frac{D_i^{1-\alpha_i} - D_{i-1}^{1-\alpha_i}}{1-\alpha_i} = \frac{M(\boldsymbol{\sigma}_i)}{\theta}\frac{2^{\theta+1}[1-\mathrm{sign}(R_{\mathrm{p}})[|R_{\mathrm{p}}|^{\mathrm{sign}(R_{\mathrm{p}}+1)}]^{\theta}]_i}{{A_{\mathrm{II}_i}}^{-\theta}[1-\mathrm{sign}(R_{\mathrm{p}})|R_{\mathrm{p}}|^{\mathrm{sign}(R_{\mathrm{p}}+1)}]_i^{\theta}}N_i \tag{15}$$

The above integration operation and similar ones below are carried out over the generic loading block $i$ of $N_i$ cycles. $D_{i-1}$ and $D_i$, respectively, denote the damage variable at the beginning and at the end of the cycle. To determine the functional form of $M$, a multiaxial fatigue criterion has to be chosen first. Since the damage evolution (15) is expressed in $A_{\mathrm{II}}$, Sines and Crossland criteria are quite suitable. Assuming the applicability of Sines criterion, two specific cyclic loadings are parameterized such that their fatigue lives, denoted by $N_{\mathrm{F_1}}$ and $N_{\mathrm{F_2}}$, are identical according to Sines fatigue criterion. Then, the mathematical expressions of these two fatigue lives are equated to obtain the functional form of $M_{\mathrm{Sns}}(\boldsymbol{\sigma})$. Further below, explanations are provided as to why these two particular choices are made.

Load configuration 1 according to Sines fatigue criterion:

$$A^{*}_{\mathrm{Sns}} = \sigma_{1_0}, \quad A_{\mathrm{II}} = \lim_{\varepsilon\to 0^{+}}(A^{*}_{\mathrm{Sns}} + \varepsilon),$$

$$\Rightarrow 1 - \alpha_{\mathrm{Sns}} = a\left(\frac{\langle A_{\mathrm{II}} - A^{*}_{\mathrm{Sns}}\rangle}{\sigma_{\mathrm{u}} - \sigma_{\mathrm{eq_M}}}\right)^{\zeta} = \lim_{\varepsilon\to 0^{+}} a\left(\frac{\varepsilon}{\sigma_{\mathrm{u}} - \sigma_{\mathrm{eq_M}}}\right)^{\zeta} \tag{16a}$$

Load configuration 2 according to Sines fatigue criterion:

$$A^{*}_{\mathrm{Sns}} = \sigma_{1_0}(1-3b\bar{\sigma}_{\mathrm{H}}), \quad A_{\mathrm{II}} = \lim_{\varepsilon\to 0^{+}}(A^{*}_{\mathrm{Sns}} + \varepsilon),$$

$$\Rightarrow 1 - \alpha_{\mathrm{Sns}} = a\left(\frac{\langle A_{\mathrm{II}} - A^{*}_{\mathrm{Sns}}\rangle}{\sigma_{\mathrm{u}} - \sigma_{\mathrm{eq_M}}}\right)^{\zeta} = \lim_{\varepsilon\to 0^{+}} a\left(\frac{\varepsilon}{\sigma_{\mathrm{u}} - \sigma_{\mathrm{eq_M}}}\right)^{\zeta} \tag{16b}$$

The first choice of load configuration is the uniaxial, symmetric fatigue loading, with the amplitude $A_{\mathrm{II}} = \sigma_{\mathrm{a}} = \lim_{\varepsilon\to 0^{+}}(\sigma_{1_0} + \varepsilon)$ and mean stress $\bar{\sigma}_{\mathrm{H}} = 0$, for which the number of cycles to failure is calculated by proper substitution into the second

relationship (15).

$$N_{\mathrm{F_1}} = \lim_{\varepsilon\to 0}\left(1 - D_0^{\,a\left(\frac{\varepsilon}{\sigma_{\mathrm{u}}-\sigma_{\mathrm{l}_0}-\varepsilon}\right)^{\zeta}}\right)\left(\frac{\varepsilon}{\sigma_{\mathrm{u}}-\sigma_{\mathrm{l}_0}-\varepsilon}\right)^{-\zeta}\frac{\theta}{4M_0\sigma_{\mathrm{l}_0}^{\theta}a} = \frac{-\theta\ln D_0}{4M_0\sigma_{\mathrm{l}_0}^{\theta}} \tag{17}$$

In the above expression, $M_0$ corresponds to the value of $M$ function at zero mean hydrostatic stress, and $D_0$ denotes the initial damage available in the specimen before fatigue loading. The significance of this model parameter is discussed further below. The second choice of load configuration corresponds to a single-block, multiaxial, harmonic one where $\bar{\sigma}_{\mathrm{H}} \neq 0$ takes any general value and $A_{\mathrm{II}} = \lim_{\varepsilon\to 0^+}\sigma_{\mathrm{l}_0}(1-3b\bar{\sigma}_{\mathrm{H}}) + \varepsilon$. Note that the octahedral shear stress amplitude is tuned with respect to the chosen fatigue criterion. The number of cycles to failure of such a load configuration is calculated by proper substitution into the damage evolution expression (15).

$$N_{\mathrm{F_2}} = \lim_{\varepsilon\to 0^+}\frac{\theta[1-\mathrm{sign}(R_{\mathrm{p}})|R_{\mathrm{p}}|^{\mathrm{sign}(R_{\mathrm{p}}+1)}]^{\theta}\left(1-D_0^{\,a\left(\frac{\varepsilon}{\sigma_{\mathrm{u}}-\sigma_{\mathrm{eq}}}\right)^{\zeta}}\right)\left(\frac{\varepsilon}{\sigma_{\mathrm{u}}-\sigma_{\mathrm{eq}}}\right)^{-\zeta}}{2^{\theta+1}aM_{\mathrm{Sns}}(\boldsymbol{\sigma})(\sigma_{\mathrm{l}_0}(1-3b\bar{\sigma}_{\mathrm{H}})+\varepsilon)^{\theta}[1-\mathrm{sign}(R_{\mathrm{p}})[|R_{\mathrm{p}}|^{\mathrm{sign}(R_{\mathrm{p}}+1)}]^{\theta}]}$$
$$= \frac{-\theta\ln D_0[1-\mathrm{sign}(R_{\mathrm{p}})|R_{\mathrm{p}}|^{\mathrm{sign}(R_{\mathrm{p}}+1)}]^{\theta}}{2^{\theta+1}M_{\mathrm{Sns}}(\boldsymbol{\sigma})(\sigma_{\mathrm{l}_0}(1-3b\bar{\sigma}_{\mathrm{H}}))^{\theta}[1-\mathrm{sign}(R_{\mathrm{p}})[|R_{\mathrm{p}}|^{\mathrm{sign}(R_{\mathrm{p}}+1)}]^{\theta}]} \tag{18}$$

The two fatigue lives calculated in Eqs. (17) and (18) belong to the loci of the points of identical fatigue lives, according to Sines criterion. For this reason, they are equated to calculate the sought-for functional form of $M_{\mathrm{Sns}}(\boldsymbol{\sigma})$.

$$M_{\mathrm{Sns}}(\boldsymbol{\sigma}) = \frac{M_0[1-\mathrm{sign}(R_{\mathrm{p}})|R_{\mathrm{p}}|^{\mathrm{sign}(R_{\mathrm{p}}+1)}]^{\theta}}{2^{\theta-1}(1-3b\bar{\sigma}_{\mathrm{H}})^{\theta}[1-\mathrm{sign}(R_{\mathrm{p}})[|R_{\mathrm{p}}|^{\mathrm{sign}(R_{\mathrm{p}}+1)}]^{\theta}]} \tag{19}$$

To comply with Chaboche's suggestion to increase the flexibility of the model, an independent model parameter $b_2$ is considered for $M_{\mathrm{Sns}}$ [46]. Substituting thus calculated $M_{\mathrm{Sns}}$ into Eq. (15) yields

$$D_i^{1-\alpha_i} - D_{i-1}^{1-\alpha_i} = (1-\alpha_i)\frac{4M_0{A_{\mathrm{II}_i}}^{\theta}}{\theta(1-3b_2\bar{\sigma}_{\mathrm{H}_i})^{\theta}}N_i$$
$$\text{where } \alpha_i = 1 - a\left(\frac{A_{\mathrm{II}_i}-\sigma_{\mathrm{l}_0}(1-3b_1\bar{\sigma}_{\mathrm{H}_i})}{\sigma_{\mathrm{u}}-\sigma_{\mathrm{eq}_{\mathrm{M}_i}}}\right)^{\zeta} \tag{20}$$

This is the HCF part of Sines$-H_{(\mathrm{i})}$ variant where $0<\alpha<1$ because $A_{\mathrm{II}_i}-\sigma_{\mathrm{l}_0}(1-3b_1\bar{\sigma}_{\mathrm{H}_i})>0$ or equivalently $A_{\mathrm{II}_i}-A^*_{\mathrm{Sns}_{(\mathrm{i})}}>0$.

$$D_i^{a\left(\frac{A_{\mathrm{II}_i}-A^*_{\mathrm{Sns}_i}}{\sigma_{\mathrm{u}}-\sigma_{\mathrm{eq}_{\mathrm{M}_i}}}\right)^{\zeta}} - D_{i-1}^{a\left(\frac{A_{\mathrm{II}_i}-A^*_{\mathrm{Sns}_i}}{\sigma_{\mathrm{u}}-\sigma_{\mathrm{eq}_{\mathrm{M}_i}}}\right)^{\zeta}} = a\left(\frac{A_{\mathrm{II}_i}-A^*_{\mathrm{Sns}_i}}{\sigma_{\mathrm{u}}-\sigma_{\mathrm{eq}_{\mathrm{M}_i}}}\right)^{\zeta}\frac{4M_0{A_{\mathrm{II}_i}}^{\theta}}{\theta(1-3b_2\bar{\sigma}_{\mathrm{H}_i})^{\theta}}N_i$$
$$\text{if } A_{\mathrm{II}_i}-A^*_{\mathrm{Sns}_{(\mathrm{i})}}>0 \tag{21}$$

Before dealing with the VHCF part of this variant, let us take a closer look at relation (21). As discussed by Chaboche, the parameter $a$ of $\alpha$ function cannot be independently identified merely by using fatigue tests [19]. It is also the case for the parameter $a$ that appears in Eq. (21) of Sines-$H_{(\mathrm{i})}$ variant and also in all other variants of the proposed DAM in this work. Although non-identifiable with HCF tests, parameter $a$ poses no problem in employing different DAM variants, as demonstrated below.

Let us introduce the new variable $\lambda_i = D_i^a$, which maps $0<D_i<1$ into $0<D_i^a=\lambda_i<1$, and the new model parameter $\eta = 4M_0a$. As such, the HCF part of Sines-$H_{(\mathrm{i})}$ variant is recast as follows, thereby eliminating parameter $a$ from expression (21).

$$\lambda_i^{\left(\frac{A_{\mathrm{II}_i}-A^*_{\mathrm{Sns}_i}}{\sigma_{\mathrm{u}}-\sigma_{\mathrm{eq}_{\mathrm{M}_i}}}\right)^{\zeta}} - \lambda_{i-1}^{\left(\frac{A_{\mathrm{II}_i}-A^*_{\mathrm{Sns}_i}}{\sigma_{\mathrm{u}}-\sigma_{\mathrm{eq}_{\mathrm{M}_i}}}\right)^{\zeta}} = \left(\frac{A_{\mathrm{II}_i}-A^*_{\mathrm{Sns}_i}}{\sigma_{\mathrm{u}}-\sigma_{\mathrm{eq}_{\mathrm{M}_i}}}\right)^{\zeta}\frac{\eta{A_{\mathrm{II}_i}}^{\theta}}{\theta(1-3b_2\bar{\sigma}_{\mathrm{H}_i})^{\theta}}N_i \tag{22}$$
$$\text{if } A_{\mathrm{II}_i}-A^*_{\mathrm{Sns}_{(\mathrm{i})}}>0$$

This new form of representation reduces the number of model parameters by one. This same idea is applied to other variants of the model in order to make parameter $a$ disappear and reduce the number of model parameters without losing its generality. It is worthwhile to recall that as explained by Lemaitre and Chaboche, "$D=0$ corresponds to the nondamaged or virgin state, $D=1$ corresponds to the breaking of the volume element into two parts …, $0<D<1$ characterizes the damaged state." (see Ref. [47]). This convention has been adopted by many researchers working in this domain, such as Refs. [20–24], among others.

*2.1.2 Sines-$H_{(i)}$ Variant—VHCF Part ($\alpha=1$).* When the expression between Macaulay brackets is no more positive, i.e., $A_{\mathrm{II}_i}-\sigma_{\mathrm{l}_0}(1-3b_1\bar{\sigma}_{\mathrm{H}_i})\leq 0$, then $\alpha=1$ and the VHCF regime is concerned. For this part of the variant, one needs to let $\alpha=1$ in Eq. (15) before calculating the integral. Since function $M$ depends exclusively on the adopted criterion, one only needs to substitute $M_{\mathrm{Sns}}$ from Eq. (19) into the right-hand side of Eq. (15). Therefore, the VHCF part of Sines-$H_{(\mathrm{i})}$ variant reads

$$\int_{D_{i-1}}^{D_i}\frac{\mathrm{d}D}{D} = \int_0^{N_i}\frac{2M(\boldsymbol{\sigma})}{\theta}\frac{(2A_{\mathrm{II}_i})^{\theta}[1-\mathrm{sign}(R_{\mathrm{p}})[|R_{\mathrm{p}}|^{\mathrm{sign}(R_{\mathrm{p}}+1)}]^{\theta}]_i}{[1-\mathrm{sign}(R_{\mathrm{p}})|R_{\mathrm{p}}|^{\mathrm{sign}(R_{\mathrm{p}}+1)}]_i^{\theta}}\mathrm{d}N$$
$$\Rightarrow \ln(D_i)-\ln(D_{i-1}) = \frac{4M_0{A_{\mathrm{II}_i}}^{\theta}}{\theta(1-3b_2\bar{\sigma}_{\mathrm{H}_i})^{\theta}}N_i \tag{23}$$

To be consistent with the variables and parameters of the HCF part in Eq. (22), the second relationship of Eq. (23) is multiplied through by $a$ which is then passed into the logarithmic expressions. Therefore, the complementary part of the variant under consideration reads

$$\ln(\lambda_i)-\ln(\lambda_{i-1}) = \frac{\eta{A_{\mathrm{II}_i}}^{\theta}}{\theta(1-3b_2\bar{\sigma}_{\mathrm{H}_i})^{\theta}}N_i \tag{24}$$

For all practical purposes, the expressions of both parts of the variant are collected in a system of equations describing Sines-$H_{(\mathrm{i})}$ variant of the DAM of the present work.

$$\begin{cases}\lambda_i^{\left(\frac{A_{\mathrm{II}_i}-A^*_{\mathrm{Sns}_i}}{\sigma_{\mathrm{u}}-\sigma_{\mathrm{eq}_{\mathrm{M}_i}}}\right)^{\zeta}} - \lambda_{i-1}^{\left(\frac{A_{\mathrm{II}_i}-A^*_{\mathrm{Sns}_i}}{\sigma_{\mathrm{u}}-\sigma_{\mathrm{eq}_{\mathrm{M}_i}}}\right)^{\zeta}} = \left(\frac{A_{\mathrm{II}_i}-A^*_{\mathrm{Sns}_i}}{\sigma_{\mathrm{u}}-\sigma_{\mathrm{eq}_{\mathrm{M}_i}}}\right)^{\zeta}\frac{\eta{A_{\mathrm{II}_i}}^{\theta}N_i}{\theta(1-3b_2\bar{\sigma}_{\mathrm{H}_i})^{\theta}} & \text{if } A_{\mathrm{II}_i}-A^*_{\mathrm{Sns}_{(\mathrm{i})}}>0\\ \ln(\lambda_i)-\ln(\lambda_{i-1}) = \frac{\eta{A_{\mathrm{II}_i}}^{\theta}N_i}{\theta(1-3b_2\bar{\sigma}_{\mathrm{H}_i})^{\theta}} & \text{if } A_{\mathrm{II}_i}-A^*_{\mathrm{Sns}_{(\mathrm{i})}}\leq 0\end{cases} \tag{25}$$

Note that when $\lambda=1$, it means that $D=1$ and the mechanical component is regarded as fully damaged. An identical derivation procedure is followed for Crossland-$H_{(\mathrm{i})}$ variant in Sec. 2.1.3.

*2.1.3 Crossland-$H_{(i)}$ Variant—High Cycle Fatigue Part ($0<\alpha<1$).* Given that Crossland fatigue criterion is expressed in terms of $A_{\mathrm{II}}$, similar to Sines criterion, Eq. (15) is the suitable form of our DAM for calculating the explicit expression of HCF part of Crossland-$H_{(\mathrm{i})}$ variant. Similar to Sines-$H_{(\mathrm{i})}$ variant, two load configurations have to be defined with respect to Crossland fatigue criterion to calculate the corresponding $N_{\mathrm{F_1}}$ and $N_{\mathrm{F_2}}$ in the first place and then find the associated $M_{\mathrm{CL}}(\boldsymbol{\sigma})$. The pair of load configurations proper to Crossland fatigue criterion are parameterized in the same way they have been set for Sines criterion.

Load configuration 1 and 2 according to Crossland fatigue criterion are as follows:

$$A^*_{\mathrm{CL}} = \sigma_{1_0}, \quad A_{\mathrm{II}} = \lim_{\varepsilon\to 0^+}(A^*_{\mathrm{CL}}+\varepsilon),$$
$$\Rightarrow 1-\alpha_{\mathrm{CL}} = a\left(\frac{\langle A_{\mathrm{II}}-A^*_{\mathrm{CL}}\rangle}{\sigma_{\mathrm{u}}-\sigma_{\mathrm{eq_M}}}\right)^{\zeta} = \lim_{\varepsilon\to 0^+} a\left(\frac{\varepsilon}{\sigma_{\mathrm{u}}-\sigma_{1_0}-\varepsilon}\right)^{\zeta} \tag{26a}$$

$$A^*_{\mathrm{CL}} = \sigma_{1_0}\frac{1-3b\sigma_{\mathrm{H_M}}}{1-b\sigma_{1_0}}, \quad A_{\mathrm{II}} = \lim_{\varepsilon\to 0^+}(A^*_{\mathrm{CL}}+\varepsilon),$$
$$\Rightarrow 1-\alpha_{\mathrm{CL}} = a\left(\frac{\langle A_{\mathrm{II}}-A^*_{\mathrm{CL}}\rangle}{\sigma_{\mathrm{u}}-\sigma_{\mathrm{eq_M}}}\right)^{\zeta} = \lim_{\varepsilon\to 0^+} a\left(\frac{\varepsilon}{\sigma_{\mathrm{u}}-\sigma_{\mathrm{eq_M}}}\right)^{\zeta} \tag{26b}$$

Following a similar procedure to Sines-$H_{(\mathrm{i})}$ variant, one obtains

$$M_{\mathrm{CL}}(\boldsymbol{\sigma}) = \frac{M_0[1-\mathrm{sign}(R_{\mathrm{p}})|R_{\mathrm{p}}|^{\mathrm{sign}(R_{\mathrm{p}}+1)}]^{\theta}}{2^{\theta-1}[1-\mathrm{sign}(R_{\mathrm{p}})[|R_{\mathrm{p}}|^{\mathrm{sign}(R_{\mathrm{p}}+1)}]^{\theta}]}\left(\frac{1-3b_2\sigma_{\mathrm{H_M}}}{1-b_2\sigma_{1_0}}\right)^{-\theta} \tag{27}$$

leading to

$$D_i^{1-\alpha_i} - D_{i-1}^{1-\alpha_i} = (1-\alpha_i)\frac{4M_0N_i{A_{\mathrm{II}_i}}^{\theta}}{\theta}\left(\frac{1-3b_2\sigma_{\mathrm{H_{M_i}}}}{1-b_2\sigma_{1_0}}\right)^{-\theta}$$
$$\text{where } \alpha_i = 1-a\left(\frac{A_{\mathrm{II}_i}-A^*_{\mathrm{CL}_i}}{\sigma_{\mathrm{u}}-\sigma_{\mathrm{eq_{M_i}}}}\right)^{\zeta} \tag{28}$$

or equivalently

$$D_i^{a\left(\frac{A_{\mathrm{II}_i}-A^*_{\mathrm{CL}_i}}{\sigma_{\mathrm{u}}-\sigma_{\mathrm{eq_{M_i}}}}\right)^{\zeta}} - D_{i-1}^{a\left(\frac{A_{\mathrm{II}_i}-A^*_{\mathrm{CL}_i}}{\sigma_{\mathrm{u}}-\sigma_{\mathrm{eq_{M_i}}}}\right)^{\zeta}} = \left(\frac{A_{\mathrm{II}_i}-A^*_{\mathrm{CL}_i}}{\sigma_{\mathrm{u}}-\sigma_{\mathrm{eq_{M_i}}}}\right)^{\zeta}\left(\frac{1-3b_2\sigma_{\mathrm{H_{M_i}}}}{1-b_2\sigma_{1_0}}\right)^{-\theta} \times \frac{4aM_0{A_{\mathrm{II}_i}}^{\theta}N_i}{\theta} \quad \text{if } A_{\mathrm{II}_i}-A^*_{\mathrm{CL}_i}>0 \tag{29}$$

since $A_{\mathrm{II}_i}-A^*_{\mathrm{CL}_i}\geq 0$. In a similar manner to Sines-$H_{(\mathrm{i})}$ variant, and using the previously introduced variable $\lambda$ and parameter $\eta$, one obtains the following more compact form, thus making parameter $a$ disappear.

$$\lambda_i^{\left(\frac{A_{\mathrm{II}_i}-A^*_{\mathrm{CL}_i}}{\sigma_{\mathrm{u}}-\sigma_{\mathrm{eq_{M_i}}}}\right)^{\zeta}} - \lambda_{i-1}^{\left(\frac{A_{\mathrm{II}_i}-A^*_{\mathrm{CL}_i}}{\sigma_{\mathrm{u}}-\sigma_{\mathrm{eq_{M_i}}}}\right)^{\zeta}} = \left(\frac{A_{\mathrm{II}_i}-A^*_{\mathrm{CL}_i}}{\sigma_{\mathrm{u}}-\sigma_{\mathrm{eq_{M_i}}}}\right)^{\zeta}\left(\frac{1-3b_2\sigma_{\mathrm{H_{M_i}}}}{1-b_2\sigma_{1_0}}\right)^{-\theta}\frac{\eta{A_{\mathrm{II}_i}}^{\theta}N_i}{\theta} \quad \text{if } A_{\mathrm{II}_i}-A^*_{\mathrm{CL}_i}>0 \tag{30}$$

Similar to the previous variant, $\lambda$ and $\eta$ allow for reducing by one of the model parameters.

*2.1.4 Crossland-$H_{(i)}$ Variant—VHCF Part ($\alpha=1$).* Similar to VHCF part of Sines-$H_{(\mathrm{i})}$, relation (23) is utilized with $M_{\mathrm{CL}}$ to obtain the VHCF part of Crossland-$H_{(\mathrm{i})}$ variant in which parameter reduction idea is applied using $\lambda$ and $\eta$.

$$\ln(D_i)-\ln(D_{i-1}) = \frac{4M_0N_i{A_{\mathrm{II}_i}}^{\theta}}{\theta}\left(\frac{1-3b_2\sigma_{\mathrm{H_{M_i}}}}{1-b_2\sigma_{1_0}}\right)^{-\theta}$$
$$\equiv \ln(\lambda_i)-\ln(\lambda_{i-1}) = \frac{\eta{A_{\mathrm{II}_i}}^{\theta}N_i}{\theta}\left(\frac{1-3b_2\sigma_{\mathrm{H_{M_i}}}}{1-b_2\sigma_{1_0}}\right)^{-\theta} \tag{31}$$

In short, Crossland-$H_{(\mathrm{i})}$ variant of the damage accumulation model is composed of relations (30) and (31) describing the HCF and VHCF regimes, respectively.

$$\begin{cases} \lambda_i^{\left(\frac{A_{\mathrm{II}_i}-A^*_{\mathrm{CL}_i}}{\sigma_{\mathrm{u}}-\sigma_{\mathrm{eq_{M_i}}}}\right)^{\zeta}} - \lambda_{i-1}^{\left(\frac{A_{\mathrm{II}_i}-A^*_{\mathrm{CL}_i}}{\sigma_{\mathrm{u}}-\sigma_{\mathrm{eq_{M_i}}}}\right)^{\zeta}} = \left(\frac{A_{\mathrm{II}_i}-A^*_{\mathrm{CL}_i}}{\sigma_{\mathrm{u}}-\sigma_{\mathrm{eq_{M_i}}}}\right)^{\zeta}\left(\frac{1-3b_2\sigma_{\mathrm{H_{M_i}}}}{1-b_2\sigma_{1_0}}\right)^{-\theta}\frac{\eta{A_{\mathrm{II}_i}}^{\theta}N_i}{\theta} & \text{if } A_{\mathrm{II}_i}-A^*_{\mathrm{CL}_i}>0 \\ \ln(\lambda_i)-\ln(\lambda_{i-1}) = \left(\frac{1-3b_2\sigma_{\mathrm{H_{M_i}}}}{1-b_2\sigma_{1_0}}\right)^{-\theta}\frac{\eta{A_{\mathrm{II}_i}}^{\theta}N_i}{\theta} & \text{if } A_{\mathrm{II}_i}-A^*_{\mathrm{CL}_i}\leq 0 \end{cases} \tag{32}$$

Application of Dang Van criterion is both different from and similar to the application of Sines and Crossland criteria. It is different because Dang Van criterion is not expressed in $A_{\mathrm{II}}$, hence making the differential equation (13) non-applicable, and it is similar because the appropriate differential equation (B13) looks very much like that of Eq. (13). Moreover, the pair of load configurations are defined in a similar manner to find the equivalent $M(\boldsymbol{\sigma})$. Appendix B is dedicated to derive the differential equation (B13), which is the analog of Eq. (13).

*2.1.5 Dang Van-$H_{(i)}$ Variant—High Cycle Fatigue Part ($0<\alpha<1$).* Integrating the differential equation (B13) with $H(D)=(1-D)^{\theta}D^{\alpha}$ for loading block $i$ with $N_i$ cycles gives

$$\int_{D_{i-1}}^{D_i}\frac{\mathrm{d}D}{D^{\alpha}} = \int_0^{N_i}\frac{M(\boldsymbol{\sigma})}{\theta}{\tau_{\mathrm{a}}}^{\theta}\phi(\boldsymbol{\sigma})\mathrm{d}N \Rightarrow \frac{D_i^{1-\alpha_i}-D_{i-1}^{1-\alpha_i}}{(1-\alpha_i)} = \frac{M(\boldsymbol{\sigma}_i)\phi(\boldsymbol{\sigma}_i)}{\theta}{\tau_{\mathrm{a}}}^{\theta}N_i \tag{33}$$

where the appropriate $\alpha$ function for Dang Van criterion introduced in relation (14) is used. Although the product of the scalar functions $M(\boldsymbol{\sigma}_i)\phi(\boldsymbol{\sigma}_i)$ in Eq. (33) can be replaced with a single unknown function, they are kept as they are. The two corresponding load configurations that help to determine $M(\boldsymbol{\sigma}_i)\phi(\boldsymbol{\sigma}_i)$ are tuned as follows.

Load configuration 1 and 2 according to Dang Van fatigue criterion:

$$A^*_{\mathrm{DV}} = \frac{\sigma_{1_0}}{2}, \quad \tau_{\mathrm{a}} = \lim_{\varepsilon\to 0^+}\left(\frac{\sigma_{1_0}}{2}+\varepsilon\right),$$
$$\Rightarrow 1-\alpha_{\mathrm{DV}} = a\left(\frac{\langle\tau_{\mathrm{a}}-A^*_{\mathrm{DV}}\rangle}{\sigma_{\mathrm{u}}-\sigma_{\mathrm{eq_M}}}\right)^{\zeta} = \lim_{\varepsilon\to 0^+} a\left(\frac{\varepsilon}{\sigma_{\mathrm{u}}-\sigma_{\mathrm{eq_M}}}\right)^{\zeta} \tag{34a}$$

$$A^*_{\mathrm{DV}} = \sigma_{1_0}\frac{1-3b\sigma_{\mathrm{H_M}}}{2(1-b\sigma_{1_0})}, \quad \tau_{\mathrm{a}} = \lim_{\varepsilon\to 0^+}(A^*_{\mathrm{DV}}+\varepsilon),$$
$$\Rightarrow 1-\alpha_{\mathrm{DV}} = a\left(\frac{\langle\tau_{\mathrm{a}}-A^*_{\mathrm{DV}}\rangle}{\sigma_{\mathrm{u}}-\sigma_{\mathrm{eq_M}}}\right)^{\zeta} = \lim_{\varepsilon\to 0^+} a\left(\frac{\varepsilon}{\sigma_{\mathrm{u}}-\sigma_{\mathrm{eq_M}}}\right)^{\zeta} \tag{34b}$$

The first load configuration is plugged into Eq. (33) to calculate the corresponding number of cycles to failure $N_{\mathrm{F_1}}$.

$$N_{\mathrm{F_1}} = \lim_{\varepsilon\to 0^+}\frac{1-D_0^{a_{\mathrm{DV}}\left(\frac{\varepsilon}{\sigma_{\mathrm{u}}-\sigma_{\mathrm{eq_M}}}\right)^{\zeta}}}{a_{\mathrm{DV}}\left(\frac{\varepsilon}{\sigma_{\mathrm{u}}-\sigma_{\mathrm{eq_M}}}\right)^{\zeta}\frac{M_0}{\theta}\left(\frac{\sigma_{1_0}}{2}+\varepsilon\right)^{\theta}\phi_0} = \frac{-\ln D_0}{\frac{M_0}{\theta}\left(\frac{\sigma_{1_0}}{2}\right)^{\theta}\phi_0} \tag{35}$$

Similarly, the number of cycles to failure corresponding to the second load configuration is calculated.

$$N_{\mathrm{F_2}} = \lim_{\varepsilon\to 0^+}\theta\frac{1-D_0^{a_{\mathrm{DV}}\left(\frac{\varepsilon}{\sigma_{\mathrm{u}}-\sigma_{\mathrm{eq_M}}}\right)^{\zeta}}}{a_{\mathrm{DV}}M(\boldsymbol{\sigma})\phi(\boldsymbol{\sigma})}\left(\frac{\varepsilon}{\sigma_{\mathrm{u}}-\sigma_{\mathrm{eq_M}}}\right)^{-\zeta}\left(\frac{\sigma_{1_0}(1-3b\sigma_{\mathrm{H_M}})}{2(1-b\sigma_{1_0})}+\varepsilon\right)^{-\theta}$$
$$= \theta\frac{-\ln D_0}{M(\boldsymbol{\sigma})\phi(\boldsymbol{\sigma})}\left(\frac{\sigma_{1_0}(1-3b\sigma_{\mathrm{H_M}})}{2(1-b\sigma_{1_0})}\right)^{-\theta} \tag{36}$$

Equating the two fatigue lives gives

$$M_{\mathrm{DV}}(\boldsymbol{\sigma})\phi_{\mathrm{DV}}(\boldsymbol{\sigma}) = M_0\phi_0\left(\frac{(1-3b_2\sigma_{\mathrm{H_M}})}{1-b_2\sigma_{\mathrm{l}_0}}\right)^{-\theta} \tag{37}$$

Substituting the above result back into Eq. (33) and opting for $b_2$ coefficient different from $b_1$, we obtain the following relationship for Dang Van-$H_{(\mathrm{i})}$ variant that suits HCF regime.

$$\begin{aligned} D_i^{1-\alpha_i} - D_{i-1}^{1-\alpha_i} &= \frac{M_0\phi_0\tau_{\mathrm{a}_i}^{\theta}}{\theta}\left(\frac{1-3b_2\sigma_{\mathrm{H_{M_i}}}}{1-b_2\sigma_{\mathrm{l}_0}}\right)^{-\theta}(1-\alpha_i)N_i \\ 1-\alpha_i &= a\left(\frac{\tau_{\mathrm{a}_i}-A^*_{\mathrm{DV}_i}}{\sigma_{\mathrm{u}}-\sigma_{\mathrm{eq_{M_i}}}}\right)^{\zeta} \end{aligned} \tag{38}$$

When $0<\alpha_{\mathrm{DV}}<1$, it means $\tau_{\mathrm{a}_i}-\sigma_{\mathrm{l}_0}(1-3b\sigma_{\mathrm{H_M}})/(2(1-b\sigma_{\mathrm{l}_0}))>0$ or equivalently $\tau_{\mathrm{a}_i}-A^*_{\mathrm{DV}_i}>0$. Therefore,

$$\begin{aligned} &D_i^{a\left(\frac{\tau_{\mathrm{a}_i}-A^*_{\mathrm{DV}_i}}{\sigma_{\mathrm{u}}-\sigma_{\mathrm{eq_{M_i}}}}\right)^{\zeta}} - D_{i-1}^{a\left(\frac{\tau_{\mathrm{a}_i}-A^*_{\mathrm{DV}_i}}{\sigma_{\mathrm{u}}-\sigma_{\mathrm{eq_{M_i}}}}\right)^{\zeta}} \\ &\quad = \frac{aM_0\phi_0\tau_{\mathrm{a}_i}^{\theta}}{\theta}\left(\frac{\tau_{\mathrm{a}_i}-A^*_{\mathrm{DV}_i}}{\sigma_{\mathrm{u}}-\sigma_{\mathrm{eq_{M_i}}}}\right)^{\zeta}\left(\frac{1-3b_2\sigma_{\mathrm{H_{M_i}}}}{1-b_2\sigma_{\mathrm{l}_0}}\right)^{-\theta}N_i \\ &\qquad \text{if } \tau_{\mathrm{a}_i}-A^*_{\mathrm{DV}_i}>0 \end{aligned} \tag{39}$$

To eliminate parameter $a$, Eq. (39) is rewritten in terms of $\lambda$ and $\eta$ similar to its Sines and Crossland counterparts.

$$\begin{aligned} &\lambda_i^{\left(\frac{\tau_{\mathrm{a}_i}-A^*_{\mathrm{DV}_i}}{\sigma_{\mathrm{u}}-\sigma_{\mathrm{eq_{M_i}}}}\right)^{\zeta}} - \lambda_{i-1}^{\left(\frac{\tau_{\mathrm{a}_i}-A^*_{\mathrm{DV}_i}}{\sigma_{\mathrm{u}}-\sigma_{\mathrm{eq_{M_i}}}}\right)^{\zeta}} \\ &\quad = \left(\frac{\tau_{\mathrm{a}_i}-A^*_{\mathrm{DV}_i}}{\sigma_{\mathrm{u}}-\sigma_{\mathrm{eq_{M_i}}}}\right)^{\zeta}\left(\frac{1-3b_2\sigma_{\mathrm{H_{M_i}}}}{1-b_2\sigma_{\mathrm{l}_0}}\right)^{-\theta}\frac{\eta\tau_{\mathrm{a}_i}^{\theta}N_i}{\theta} \quad \text{if } \tau_{\mathrm{a}_i}-A^*_{\mathrm{DV}_i}>0 \end{aligned} \tag{40}$$

*2.1.6 Dang Van-$H_{(i)}$ Variant—VHCF Part ($\alpha=1$).* The complementary part of the current variant for the VHCF regime is obtained by setting $\alpha=1$.

$$\begin{aligned} \int_{D_{i-1}}^{D_i}\frac{\mathrm{d}D}{D} &= \int_0^{N_i}\frac{M(\boldsymbol{\sigma})}{\theta}\tau_{\mathrm{a}_i}^{\theta}\phi(\boldsymbol{\sigma})\mathrm{d}N \Rightarrow \ln(D_i)-\ln(D_{i-1}) \\ &= \frac{M(\boldsymbol{\sigma}_i)\phi(\boldsymbol{\sigma}_i)}{\theta}\tau_{\mathrm{a}_i}^{\theta}N_i \end{aligned} \tag{41}$$

Substituting for $M(\boldsymbol{\sigma}_i)\phi(\boldsymbol{\sigma}_i)$ from Eqs. (37) into (41) and multiplying through by $a$ gives the following explicit expression:

$$\begin{aligned} a\ln(D_i)-a\ln(D_{i-1}) &= \frac{aM_0\phi_0}{\theta}\tau_{\mathrm{a}_i}{}^{\theta}N_i\left(\frac{1-3b_2\sigma_{\mathrm{H_{M_i}}}}{1-b_2\sigma_{\mathrm{l}_0}}\right)^{-\theta} \equiv \ln\left(\frac{\lambda_i}{\lambda_{i-1}}\right) \\ &= \frac{\eta}{\theta}\tau_{\mathrm{a}_i}{}^{\theta}N_i\left(\frac{1-3b_2\sigma_{\mathrm{H_{M_i}}}}{1-b_2\sigma_{\mathrm{l}_0}}\right)^{-\theta} \end{aligned} \tag{42}$$

For ease of reference, both parts of the Dang Van-$H_{(\mathrm{i})}$ variant are presented as follows:

$$\begin{cases} \lambda_i^{\left(\frac{\tau_{\mathrm{a}_i}-A^*_{\mathrm{DV}_i}}{\sigma_{\mathrm{u}}-\sigma_{\mathrm{eq_{M_i}}}}\right)^{\zeta}} - \lambda_{i-1}^{\left(\frac{\tau_{\mathrm{a}_i}-A^*_{\mathrm{DV}_i}}{\sigma_{\mathrm{u}}-\sigma_{\mathrm{eq_{M_i}}}}\right)^{\zeta}} \\ \quad = \left(\frac{\tau_{\mathrm{a}_i}-A^*_{\mathrm{DV}_i}}{\sigma_{\mathrm{u}}-\sigma_{\mathrm{eq_{M_i}}}}\right)^{\zeta}\left(\frac{1-3b_2\sigma_{\mathrm{H_{M_i}}}}{1-b_2\sigma_{\mathrm{l}_0}}\right)^{-\theta}\frac{\eta\tau_{\mathrm{a}_i}{}^{\theta}N_i}{\theta} & \text{if } \tau_{\mathrm{a}_i}-A^*_{\mathrm{DV}_i}>0 \\ \ln\left(\frac{\lambda_i}{\lambda_{i-1}}\right) = \frac{\eta}{\theta}\tau_{\mathrm{a}_i}{}^{\theta}N_i\left(\frac{1-3b_2\sigma_{\mathrm{H_{M_i}}}}{1-b_2\sigma_{\mathrm{l}_0}}\right)^{-\theta} & \text{if } \tau_{\mathrm{a}_i}-A^*_{\mathrm{DV}_i}\le 0 \end{cases} \tag{43}$$

In this way, three different variants of the proposed DAM, corresponding to three different multiaxial fatigue criteria, are analytically derived. For each variant, two expressions corresponding to two fatigue life regimes of HCF and VHCF are provided. Mathematical expressions of the above variants are direct functions of the adopted $H(D)$. In the following section, a different form of dependence for $H(D)$ is studied and the expressions of the new variants are subsequently determined.

**2.2 Case (ii): $H(D)=[I-(I-D)^{1+\theta}]^{\alpha}$.** With this particular choice for $H(D)$, one retrieves Chaboche's fatigue DAM [19,44] as will be demonstrated later on. This correspondence serves as a validation for our proposed DAM as it is general enough such that Chaboche's DAM for HCF and VHCF regimes is one of its innumerable variants. This is indeed the strength of the fundamental differential equations (13) and (B13) that we developed in this work as they provide the users with more degrees of freedom to examine different forms of dependence for $H(D)$ together with different fatigue criteria and then choose the one that is best suited for their application. Similar to the treatment provided under case (i), the same fatigue criteria are deployed with $H(D)$ of case (ii) to derive the analogs of the previous variants.

*2.2.1 Sines-$\mathrm{H}_{(ii)}$ Variant, High Cycle Fatigue Part ($0<\alpha<1$).* Integration of the governing differential equation (13) using the new $H(D)$ over the loading block $i$ with $N_i$ cycles to failure when $0<\alpha_i<1$, yields

$$\begin{aligned} &\int_{D_{i-1}}^{D_i}\frac{(1-D)^{\theta}\mathrm{d}D}{[1-(1-D)^{\theta+1}]^{\alpha}} \\ &\quad = \int_0^{N_i}\frac{M(\boldsymbol{\sigma}_i)}{\theta}\frac{2^{\theta+1}A_{\mathrm{II}_i}{}^{\theta}[1-\mathrm{sign}(R_{\mathrm{p}})[|R_{\mathrm{p}}|^{\mathrm{sign}(R_{\mathrm{p}}+1)}]^{\theta}]_i}{[1-\mathrm{sign}(R_{\mathrm{p}})|R_{\mathrm{p}}|^{\mathrm{sign}(R_{\mathrm{p}}+1)}]_i^{\theta}}\mathrm{d}N \\ &\Rightarrow \frac{[1-(1-D_i)^{\theta+1}]^{1-\alpha_i}-[1-(1-D_{i-1})^{\theta+1}]^{1-\alpha_i}}{2^{\theta+1}(1-\alpha_i)(\theta+1)} \\ &\quad = \frac{M(\boldsymbol{\sigma}_i)}{\theta}\frac{A_{\mathrm{II}_i}{}^{\theta}[1-\mathrm{sign}(R_{\mathrm{p}})[|R_{\mathrm{p}}|^{\mathrm{sign}(R_{\mathrm{p}}+1)}]^{\theta}]_i}{[1-\mathrm{sign}(R_{\mathrm{p}})|R_{\mathrm{p}}|^{\mathrm{sign}(R_{\mathrm{p}}+1)}]_i^{\theta}}N_i \end{aligned} \tag{44}$$

As discussed earlier under case (i), determination of the functional form of $M(\boldsymbol{\sigma}_i)$ requires a fatigue criterion. It is assumed that Sines criterion applies and the two load configurations (16) are substituted into the damage equation (44) to calculate the corresponding number of cycles to failure, $N_{\mathrm{F_1}}$ and $N_{\mathrm{F_2}}$. Accordingly,

$$\begin{aligned} N_{\mathrm{F_1}} &= \lim_{\varepsilon\to 0^+}\frac{\theta}{4M_0\sigma_{\mathrm{l}_0}^{\theta}}\frac{1-[1-(1-D_0)^{\theta+1}]^{a\left(\frac{\varepsilon}{\sigma_{\mathrm{u}}-\sigma_{\mathrm{l}_0}-\varepsilon}\right)^{\zeta}}}{a\left(\frac{\varepsilon}{\sigma_{\mathrm{u}}-\sigma_{\mathrm{l}_0}-\varepsilon}\right)^{\zeta}(\theta+1)} \\ &= -\frac{\theta}{4(\theta+1)M_0\sigma_{\mathrm{l}_0}^{\theta}}\ln[1-(1-D_0)^{\theta+1}] \end{aligned} \tag{45}$$

$$\begin{aligned} N_{\mathrm{F_2}} &= \lim_{\varepsilon\to 0^+}\frac{\theta}{M(\boldsymbol{\sigma})2^{\theta+1}(\sigma_{\mathrm{l}_0}(1-3b\bar{\sigma}_{\mathrm{H}})+\varepsilon)^{\theta}}\frac{[1-\mathrm{sign}(R_{\mathrm{p}})|R_{\mathrm{p}}|^{\mathrm{sign}(R_{\mathrm{p}}+1)}]^{\theta}}{[1-\mathrm{sign}(R_{\mathrm{p}})[|R_{\mathrm{p}}|^{\mathrm{sign}(R_{\mathrm{p}}+1)}]^{\theta}]} \\ &\quad \times\frac{1-[1-(1-D_0)^{\theta+1}]^{a\left(\frac{\varepsilon}{\sigma_{\mathrm{u}}-\sigma_{\mathrm{eq_M}}}\right)^{\zeta}}}{a\left(\frac{\varepsilon}{\sigma_{\mathrm{u}}-\sigma_{\mathrm{eq_M}}}\right)^{\zeta}(\theta+1)} \\ &= -\frac{\theta\ln[1-(1-D_0)^{\theta+1}]}{(\theta+1)M(\boldsymbol{\sigma})2^{\theta+1}(\sigma_{\mathrm{l}_0}(1-3b\bar{\sigma}_{\mathrm{H}}))^{\theta}}\frac{[1-\mathrm{sign}(R_{\mathrm{p}})|R_{\mathrm{p}}|^{\mathrm{sign}(R_{\mathrm{p}}+1)}]^{\theta}}{[1-\mathrm{sign}(R_{\mathrm{p}})[|R_{\mathrm{p}}|^{\mathrm{sign}(R_{\mathrm{p}}+1)}]^{\theta}]} \end{aligned} \tag{46}$$

Equating both fatigue lives gives $M_{\mathrm{Sns}}(\boldsymbol{\sigma})$.

$$M_{\mathrm{Sns}}(\boldsymbol{\sigma}) = \frac{M_0}{2^{\theta-1}(1-3b\bar{\sigma}_{\mathrm{H}})^{\theta}} \frac{[1-\mathrm{sign}(R_{\mathrm{p}})|R_{\mathrm{p}}|^{\mathrm{sign}(R_{\mathrm{p}}+1)}]^{\theta}}{[1-\mathrm{sign}(R_{\mathrm{p}})[|R_{\mathrm{p}}|^{\mathrm{sign}(R_{\mathrm{p}}+1)}]^{\theta}]} \tag{47}$$

A quick check with $M_{\mathrm{Sns}}(\boldsymbol{\sigma})$ of Eq. (19), which is obtained with $H(D)$ of case (i), shows that both expressions are essentially identical. This identity seems limited to these two cases examined here. Substitution of $M_{\mathrm{Sns}}$ into Eq. (44) gives the explicit expression of the Sines-$H_{(\mathrm{ii})}$ variant of our DAM for HCF regime.

$$\begin{aligned}
&\frac{[1-(1-D_i)^{\theta+1}]^{1-\alpha_i} - [1-(1-D_{i-1})^{\theta+1}]^{1-\alpha_i}}{1-\alpha_i} \\
&= \frac{4(\theta+1)M_0}{\theta} \frac{{A_{\mathrm{II}_i}}^{\theta}}{(1-3b_2\bar{\sigma}_{\mathrm{H}_i})^{\theta}} N_i \\
&\text{where } 1-\alpha_i = a\left(\frac{A_{\mathrm{II}_i} - \sigma_{\mathrm{l}_0}(1-3b_1\bar{\sigma}_{\mathrm{H}_i})}{\sigma_{\mathrm{u}} - \sigma_{\mathrm{eq}_{\mathrm{M}_i}}}\right)^{\zeta}
\end{aligned} \tag{48}$$

To eliminate parameter $a$, the equivalence between the following inequalities is exploited.

$$0 < D < 1 \equiv 0 < (1-D)^{1+\theta} < 1 \equiv 0 < [1-(1-D)^{1+\theta}]^{a} < 1 \tag{49}$$

Therefore, a new model parameter $\mu = 4M_0(1+\theta)a$, corresponding to $\eta$, together with a new variable $\delta = [1-(1-D)^{1+\theta}]^{a}$, corresponding to $\lambda$, are introduced here to rewrite relation (48) into the following shorter form.

$$\begin{aligned}
&\delta_i^{\left(\frac{A_{\mathrm{II}_i} - A^*_{\mathrm{Sns}_i}}{\sigma_{\mathrm{u}} - \sigma_{\mathrm{eq}_{\mathrm{M}_i}}}\right)^{\zeta}} - \delta_{i-1}^{\left(\frac{A_{\mathrm{II}_i} - A^*_{\mathrm{Sns}_i}}{\sigma_{\mathrm{u}} - \sigma_{\mathrm{eq}_{\mathrm{M}_i}}}\right)^{\zeta}} = \left(\frac{A_{\mathrm{II}_i} - A^*_{\mathrm{Sns}_i}}{\sigma_{\mathrm{u}} - \sigma_{\mathrm{eq}_{\mathrm{M}_i}}}\right)^{\zeta} \frac{\mu {A_{\mathrm{II}_i}}^{\theta} N_i}{\theta(1-3b_2\bar{\sigma}_{\mathrm{H}_i})^{\theta}} \\
&\text{if } A_{\mathrm{II}_i} - A^*_{\mathrm{Sns}_{(\mathrm{i})}} > 0
\end{aligned} \tag{50}$$

A quick check with the HCF part of Sines-$H_{(\mathrm{i})}$ variant shows that both expressions (22) and (50) are essentially identical, implying that for a given multiaxial fatigue criterion, both cases (i) and (ii) for $H(D)$ lead to the same damage accumulation rule. This conclusion is also true for the VHCF part of this variant, as is shown below.

*2.2.2 Sines-$H_{(ii)}$ Variant, VHCF Part ($\alpha = 1$).* Following a similar procedure, one obtains

$$\begin{aligned}
&\int_{D_{i-1}}^{D_i} \frac{(1-D)^{\theta}\mathrm{d}D}{1-(1-D)^{\theta+1}} \\
&= \int_0^{N_i} \frac{2M(\boldsymbol{\sigma})}{\theta} \frac{(2A_{\mathrm{II}_i})^{\theta}[1-\mathrm{sign}(R_{\mathrm{p}})[|R_{\mathrm{p}}|^{\mathrm{sign}(R_{\mathrm{p}}+1)}]^{\theta}]_i}{[1-\mathrm{sign}(R_{\mathrm{p}})|R_{\mathrm{p}}|^{\mathrm{sign}(R_{\mathrm{p}}+1)}]_i^{\theta}} \mathrm{d}N \\
&\Rightarrow \ln[1-(1-D_i)^{\theta+1}] - \ln[1-(1-D_{i-1})^{\theta+1}] \\
&= \frac{4(1+\theta)M_0 {A_{\mathrm{II}_i}}^{\theta}}{\theta(1-3b_2\bar{\sigma}_{\mathrm{H}_i})^{\theta}} N_i
\end{aligned} \tag{51}$$

Multiplying through by $a$ and making use of the newly defined parameter $\mu$ and variable $\delta$, the VHCF part of Sines-$H_{(\mathrm{ii})}$ variant takes the following new form of representation.

$$\ln \delta_i - \ln \delta_{i-1} = \frac{\mu {A_{\mathrm{II}_i}}^{\theta} N_i}{\theta(1-3b_2\bar{\sigma}_{\mathrm{H}_i})^{\theta}} \tag{52}$$

It can be seen that both expressions (24) and (52) are in fact identical. This correspondence as well as other similar ones implies that only when HCF and/or VHCF loadings are involved, both choices of $H(D)$ give rise to the same mathematical expressions of the damage accumulation rule for a given fatigue criterion. This is however not the case if other damage mechanisms, such as creep loading, are also active because in that case parameter $a$ remains as an independently identifiable parameter that cannot be eliminated as is done in this work.

*2.2.3 Crossland-$H_{(ii)}$ Variant, High Cycle Fatigue ($\alpha < 1$) and VHCF ($\alpha = 1$) Parts.* Assuming the applicability of Crossland criterion, one has to consider the load configurations (26) in combination with the relationship (44) to obtain $M_{\mathrm{CL}}$.

$$M_{\mathrm{CL}}(\boldsymbol{\sigma}) = \frac{M_0[1-\mathrm{sign}(R_{\mathrm{p}})|R_{\mathrm{p}}|^{\mathrm{sign}(R_{\mathrm{p}}+1)}]^{\theta}}{2^{\theta-1}\left(\frac{1-3b_2\sigma_{\mathrm{H_M}}}{1-b_2\sigma_{\mathrm{l}_0}}\right)^{\theta}[1-\mathrm{sign}(R_{\mathrm{p}})[|R_{\mathrm{p}}|^{\mathrm{sign}(R_{\mathrm{p}}+1)}]^{\theta}]} \tag{53}$$

As is the case for $M_{\mathrm{Sns}}$, $M_{\mathrm{CL}}$ too looks independent of the mathematical form of $H(D)$. Therefore, Crossland-$H_{(\mathrm{ii})}$ variant of the proposed DAM for HCF regime reads

$$\begin{aligned}
&\delta_i^{\left(\frac{A_{\mathrm{II}_i} - A^*_{\mathrm{CL}_i}}{\sigma_{\mathrm{u}} - \sigma_{\mathrm{eq}_{\mathrm{M}_i}}}\right)^{\zeta}} - \delta_{i-1}^{\left(\frac{A_{\mathrm{II}_i} - A^*_{\mathrm{CL}_i}}{\sigma_{\mathrm{u}} - \sigma_{\mathrm{eq}_{\mathrm{M}_i}}}\right)^{\zeta}} \\
&= \frac{\mu {A_{\mathrm{II}_i}}^{\theta}}{\theta}\left(\frac{1-3b_2\sigma_{\mathrm{H_{M_i}}}}{1-b_2\sigma_{\mathrm{l}_0}}\right)^{-\theta}\left(\frac{A_{\mathrm{II}_i} - A^*_{\mathrm{CL}_i}}{\sigma_{\mathrm{u}} - \sigma_{\mathrm{eq}_{\mathrm{M}_i}}}\right)^{\zeta} N_i \quad \text{if } A_{\mathrm{II}_i} - A^*_{\mathrm{CL}_i} > 0
\end{aligned} \tag{54}$$

in which use is made of newly defined parameter $\mu$ and variable $\delta$. Likewise, the VHCF part of Crossland-$H_{(\mathrm{ii})}$ variant is obtained as:

$$\ln(\delta_i) - \ln(\delta_{i-1}) = \frac{\mu {A_{\mathrm{II}_i}}^{\theta} N_i}{\theta}\left(\frac{1-3b_2\sigma_{\mathrm{H_{M_i}}}}{1-b_2\sigma_{\mathrm{l}_0}}\right)^{-\theta} \quad \text{if } A_{\mathrm{II}_i} - A^*_{\mathrm{CL}_i} \le 0 \tag{55}$$

It can be seen that Eqs. (54) and (55) are identical to their corresponding ones in Eqs. (30) and (31), which are obtained with $H_{(\mathrm{i})}$.

*2.2.4 Dang Van-$H_{(ii)}$ Variant, High Cycle Fatigue ($\alpha < 1$) and VHCF ($\alpha = 1$) Parts.* By following a similar procedure, the mathematical expressions of both parts of Dang Van-$H_{(\mathrm{ii})}$ variant are determined. Factoring out the intermediate mathematical steps leading to these two expressions, one finally obtains

$$\begin{cases}
\delta_i^{\left(\frac{\tau_{\mathrm{a}_i} - A^*_{\mathrm{DV}_i}}{\sigma_{\mathrm{u}} - \sigma_{\mathrm{eq}_{\mathrm{M}_i}}}\right)^{\zeta}} - \delta_{i-1}^{\left(\frac{\tau_{\mathrm{a}_i} - A^*_{\mathrm{DV}_i}}{\sigma_{\mathrm{u}} - \sigma_{\mathrm{eq}_{\mathrm{M}_i}}}\right)^{\zeta}} \\
\quad = \frac{\mu \tau_{\mathrm{a}_i}^{\theta} N_i}{\theta}\left(\frac{\tau_{\mathrm{a}_i} - A^*_{\mathrm{DV}_i}}{\sigma_{\mathrm{u}} - \sigma_{\mathrm{eq}_{\mathrm{M}_i}}}\right)^{\zeta}\left(\frac{1-3b_2\sigma_{\mathrm{H_{M_i}}}}{1-b_2\sigma_{\mathrm{l}_0}}\right)^{-\theta} & \text{if } \tau_{\mathrm{a}_i} - A^*_{\mathrm{DV}_i} > 0 \\
\ln\left(\frac{\delta_i}{\delta_{i-1}}\right) = \frac{\mu}{\theta}\tau_{\mathrm{a}_i}^{\theta} N_i \left(\frac{1-3b_2\sigma_{\mathrm{H_{M_i}}}}{1-b_2\sigma_{\mathrm{l}_0}}\right)^{-\theta} & \text{if } \tau_{\mathrm{a}_i} - A^*_{\mathrm{DV}_i} \le 0
\end{cases} \tag{56}$$

Again, the corresponding expressions of both Dang Van variants are technically identical.

## 3 Parameter Identification of the Damage Accumulation Model Variants Using the Uniaxial Form

To explain the efficient identification scheme devised here for the model parameters of this study, let us take as example, Sines-$H_{(\mathrm{i})}$ variant of the multiaxial DAM presented in Eq. (25). The HCF part of this variant is first reduced to uniaxial loading conditions, merely because the simplest fatigue tests to perform in the laboratory are single-block, uniaxial HCF tests with different values for mean stress $\bar{\sigma}$ and stress amplitude $\sigma_{\mathrm{a}}$. In each fatigue test, $\bar{\sigma}_{\mathrm{H}} = \bar{\sigma}/3$ and $A_{\mathrm{II}} = \sigma_{\mathrm{a}}$ are imposed as test variables (inputs) and the corresponding number of cycles to failure $N_{\mathrm{F}}$ are counted (output). In this way, an experimental fatigue test database is prepared from

which the parameters of the variant in question developed for multiaxial proportional loadings should be identified. Solving the HCF part of Sines-$H_{(i)}$ variant for $N_F$ under a generic single-block, uniaxial loading reads

$$N_F = \theta\left(\frac{\sigma_a - \sigma_{l_0}(1-b_1\bar{\sigma})}{\sigma_u - \bar{\sigma} - \sigma_a}\right)^{-\zeta} \frac{1-\lambda_0^{\left(\frac{\sigma_a-\sigma_{l_0}(1-b_1\bar{\sigma})}{\sigma_u-\bar{\sigma}-\sigma_a}\right)^{\zeta}}}{\eta\sigma_a^{\theta}(1-b_2\bar{\sigma})^{-\theta}} \tag{57}$$

where $\sigma_a - \sigma_{l_0}(1-b_1\bar{\sigma}) > 0$. For a generic single-block, uniaxial HCF test, $i=1$ and $\lambda_{i-1} = \lambda_0 = D_0^a$, is a measure of the initial damage in the specimen before running the fatigue test, and $\lambda_1 = D_1^a = 1$ indicates the damage at the break where the corresponding number of cycles to failure $N_F$ is recorded. Should we take the conventional value of $10^{+7}$ cycles at $\bar{\sigma}=0$, $\sigma_a = \lim_{\varepsilon\to 0^+}\sigma_{l_0} + \varepsilon$ for defining the fatigue endurance limit,$\sigma_{l_0}$, then $\lambda_0$ is correlated with other model parameters as follows:

$$\begin{aligned}\lim_{\varepsilon\to 0^+} N_F &= \lim_{\varepsilon\to 0^+} \theta\left(\frac{\varepsilon}{\sigma_u - \bar{\sigma} - \sigma_a}\right)^{-\zeta} \frac{1-\lambda_0^{\left(\frac{\varepsilon}{\sigma_u-\bar{\sigma}-\sigma_a}\right)^{\zeta}}}{\eta(\sigma_{l_0}+\varepsilon)^{\theta}} \\ &= -\frac{\theta\ln(\lambda_0)}{\eta\sigma_{l_0}^{\theta}} \Rightarrow \lambda_0 = \exp\left(-\frac{\eta\sigma_{l_0}^{\theta}\times 10^7}{\theta}\right)\end{aligned} \tag{58}$$

This is the advantage of using parameter $\lambda_0$ that establishes a relationship between the conventional (or maybe subjective) $N_F$ corresponding to the definition of $\sigma_{l_0}$ through the right-hand side expression of Eq. (58). Furthermore, $\lambda_0$ allows for the generalization of the proposed DAM variants to other alloys than ferrous and titanium alloys. This property of the as-presented DAM variants together with the *ad hoc* identification scheme permits identifying $\sigma_{l_0}$ using fatigue tests run at $R>0$, which is the admissible range for specimens prone to buckling under $R<0$. This feature is further discussed below.

From among different identification schemes that we tested, the most successful one is set forth in the following lines. This identification scheme is explained for the case of fatigue tests with $R>0$ which is safer than HCF tests with $R<0$. This is the strength of the identification scenario adopted here as it does not require fatigue tests with $R=-1$ to determine $\sigma_{l_0}$, and this material property is treated like other model parameters to be identified.

Let us consider a sufficiently rich database of HCF tests of a material whose cumulative fatigue damage evolution is satisfactorily described by Sines-$H_{(i)}$ variant. Using the two-level parameter identification procedure that is deployed here, $\sigma_{l_0}$, $b_1$, $\eta$, $\theta$, and $\zeta$ are identified in the first level. For this stage, $\sigma_u$ and $\sigma_y$, the material's ultimate tensile strength and yield stress, respectively, are the only material properties that are required. Although being a material property, $\sigma_{l_0}$ is treated as a model parameter to identify, merely to examine the efficacy of the proposed identification scheme. With regard to $\lambda_0$, as explained earlier, it is not an independent parameter and its interrelation with other parameters is given in Eq. (58). In the second level of identification procedure, $b_2$ will be the only parameter to identify. To eliminate $b_2$ from the first level of identification, let us consider two fatigue tests $i, j$ with identical $\bar{\sigma}$. Their cycles to failure ratio ($CFR_{\text{model}}$) as predicted by relation (57) yields

$$CFR_{\text{model}} = \frac{N_{F_i}}{N_{F_j}} = \frac{\sigma_{a_j}^{\theta}\left(\frac{\sigma_{a_j}-\sigma_{l_0}(1-b_1\bar{\sigma}_j)}{\sigma_u-\bar{\sigma}_j-\sigma_{a_j}}\right)^{\zeta}}{\sigma_{a_i}^{\theta}\left(\frac{\sigma_{a_i}-\sigma_{l_0}(1-b_1\bar{\sigma}_i)}{\sigma_u-\bar{\sigma}_i-\sigma_{a_i}}\right)^{\zeta}} \frac{1-\lambda_0^{\left(\frac{\sigma_{a_i}-\sigma_{l_0}(1-b_1\bar{\sigma}_i)}{\sigma_u-\bar{\sigma}_i-\sigma_{a_i}}\right)^{\zeta}}}{1-\lambda_0^{\left(\frac{\sigma_{a_j}-\sigma_{l_0}(1-b_1\bar{\sigma}_j)}{\sigma_u-\bar{\sigma}_j-\sigma_{a_j}}\right)^{\zeta}}} \tag{59}$$

thus eliminating $b_2$ from the first level of identification, keeping in mind that $\eta$, which does not explicitly appear in $CFR_{\text{model}}$, is a function of $\sigma_{l_0}$, $\theta$, and $\lambda_0$, according to Eq. (58). Assuming $P$ batches of fatigue tests with the test batch $k$ consisting of $Q_k$ fatigue tests with identical $\bar{\sigma}_k$, then the following nonnegative scalar cost function defined in terms $CFR_{\text{model}}$ and their corresponding $CFR_{\text{test}}$ helps to carry out the first level of identification.

$$OF_1 = \sum_{k=1}^{P}\sum_{i=1}^{Q_k-1}\sum_{j=i+1}^{Q_k} \max\left\{\left|\frac{CFR_{\text{model}}}{CFR_{\text{test}}}-1\right|, \left|\frac{CFR_{\text{test}}}{CFR_{\text{model}}}-1\right|\right\} \tag{60}$$

The above objective function proved to be the most successful and most robust one after having tested various relevant objective functions. In this way, $OF_1$ is defined in terms of the first set of unknown model parameters. Obviously, for all fatigue test batches $Q_k \geq 2$ and also the number of all independent HCF tests in the fatigue database ought to be greater than five, the number of model parameters appearing in the first level. With these conditions being satisfied, the objective is searching for the global minimum of $OF_1$, which is taken as the best set of $\sigma_{l_0}$, $b_1$, $\eta$, $\theta$, and $\zeta$ for the alloy from which the fatigue database is prepared.

For the second level of identification, namely identifying $b_2$, the following nonnegative scalar objective function is defined on all fatigue tests.

$$OF_2 = \sum_{i=1}^{n} \max\left\{\left|\frac{N_{F_i\text{model}}}{N_{F_i\text{model}}}-1\right|, \left|\frac{N_{F_i\text{test}}}{N_{F_i\text{model}}}-1\right|\right\} \tag{61}$$

Theoretically, if the model parameters $\sigma_{l_0}$, $b_1$, $\eta$, $\theta$, and $\zeta$ are successfully identified in the first level and plugged into all $N_{F_i}$ model expressions in Eq. (61), $b_2$ will be readily identified from the minimization of $OF_2$. Nonetheless, we noticed that the best practice is to re-identify $\eta$ along with $b_2$ in the second level, simply to achieve a better robustness to noisy fatigue data. In this manner, the impact of noise is minimized on the identified $\eta$ and $b_2$.

To verify the performance of the proposed identification procedure, the model parameters and material properties of SM490 steel, given in Table 1, are taken from Refs. [23] and [48]. To those values, we added $\zeta$, the extra parameter of our DAM variants. So, the idea is to build an artificial HCF database using these parameters in conjunction with Eq. (57) and then employ the above-described two-level identification scheme to identify the associated model parameters. To this end, one needs to choose the appropriate pairs of $(\bar{\sigma}_i, \sigma_{a_i})$ such that the necessary inequality of Eq. (57) is satisfied and the corresponding number of cycles to failure lies $10^5 < N_{F_i} < 10^7$. Table 2 lists 30 such HCF tests, equivalent to five times the number of model parameters to identify. Note that all fatigue tests fulfill $\sigma_m > 0$ and $\sigma_M < \sigma_{ut}$ thereby $R>0$ to make sure that all tests lie in the safe region for specimens susceptible to buckling under compression ($R<0$). The HCF tests of Table 2 are sorted into six test batches based on their mean stress value.

The artificially generated data of Table 2 are used to define $OF_1$ and $OF_2$ within a MATLAB script. Running both levels of identification using Genetic Algorithm toolbox in MATLAB returns the original values of $\sigma_{l_0}$, $b_1$, $b_2$, $\eta$, $\theta$, and $\zeta$ given in Table 1 with negligibly small error. This excellent agreement is a necessary step of validation for the implemented identification procedure. Although such an agreement would have been achieved with lesser data points, to investigate the robustness of the identification procedure to noisy inputs, we opted for 30 data points, which will be subsequently perturbed with noise. To superpose the original database of Table 2 with noise, we use the following simple and physically plausible form of additive white noise

$$N'_{F_i} = N_{F_i} + \mathcal{N}(0, Var) \tag{62}$$

where $\mathcal{N}(0, Var)$ denotes a random number from the normal distribution with 0 mean and variance $Var$, which is naturally taken as a function of $N_{F_i}$. For the purpose of this investigation, we take two different values $Var = \{N_{F_i}, 100N_{F_i}\}$ for the variance and repeat superposition with noise, 2000 times followed by the two-level identification scheme outlined earlier. Hence, two clusters of 2000 noisy datasets are built where for each noisy dataset, all $N_{F_i}$ in Table 2 are replaced with their corresponding noisy $N'_{F_i}$

**Table 1 Material properties and fatigue model parameters of SM490 steel taken from Refs. [23,48]**

| $\sigma_{0.2}$ (MPa) | $\sigma_{ut}$ (MPa) | $\sigma_{l_0}$ (MPa) | $\eta$ | $\theta$ | $b_1$ (MPa)$^{-1}$ | $b_2$ (MPa)$^{-1}$ | $\zeta$ |
|---|---|---|---|---|---|---|---|
| 424 | 691 | 275 | $4.035\times10^{-9}$ | 1.581 | $2.4\times10^{-3}$ | $1.1\times10^{-4}$ | 1.6 |

**Table 2 Artificial fatigue database consisting of 30 HCF data points calculated from the pairs of ($\bar{\sigma}$, $\sigma_M$) of each point and parameters of Table 1 plugged into Eq. (57). The data points are arranged into six batches based on their $\bar{\sigma}$**

| Test batch 1, $\bar{\sigma}=240$ MPa | | Test batch 2, $\bar{\sigma}=270$ MPa | | Test batch 3, $\bar{\sigma}=300$ MPa | | Test batch 4, $\bar{\sigma}=330$ MPa | | Test batch 5, $\bar{\sigma}=360$ MPa | | Test batch 6, $\bar{\sigma}=390$ MPa | |
|---|---|---|---|---|---|---|---|---|---|---|---|
| $\sigma_M$ (MPa) | $N_F$ | $\sigma_M$ (MPa) | $N_F$ | $\sigma_M$ (MPa) | $N_F$ | $\sigma_M$ (MPa) | $N_F$ | $\sigma_M$ (MPa) | $N_F$ | $\sigma_M$ (MPa) | $N_F$ |
| 460 | 269,088 | 470 | 290,803 | 480 | 318,254 | 490 | 353,925 | 500 | 401,915 | 530 | 229,311 |
| 440 | 503,967 | 460 | 398,466 | 460 | 626,020 | 470 | 719,202 | 480 | 850,831 | 500 | 692,019 |
| 420 | 1,043,615 | 440 | 798,559 | 450 | 911,083 | 450 | 1,640,615 | 470 | 1,292,505 | 490 | 1,048,605 |
| 410 | 1,593,093 | 430 | 1,183,452 | 440 | 1,372,626 | 440 | 2,651,686 | 450 | 3,414,584 | 470 | 2,709,748 |
| 400 | 2,583,329 | 410 | 3,023,216 | 410 | 6,757,574 | 420 | 8,801,561 | 440 | 6,151,388 | 460 | 4,750,408 |

**Table 3 Mean and variance of model parameters identified from the noisy data of Table 2 perturbed with white noise. Two perturbation cases are analyzed and each is repeated 2000 times.**

| | $N'_{F_i}$ | $\sigma'_{l_0}$ (MPa) | $\eta'$ | $\theta'$ | $b'_1$ (MPa)$^{-1}$ | $b'_2$ (MPa)$^{-1}$ | $\zeta'$ |
|---|---|---|---|---|---|---|---|
| Mean | $N_{F_i}$ | 275.024 | $4.038\times10^{-9}$ | 1.5824 | $2.40\times10^{-3}$ | $1.11\times10^{-4}$ | 1.60 |
| Variance | $N_{F_i}$ | 0.606 | $2.83\times10^{-19}$ | $5.05\times10^{-4}$ | $4.076\times10^{-12}$ | $2.11\times10^{-9}$ | $1.42\times10^{-4}$ |
| Mean | $N_{F_i}$ | 275.23 | $7.904\times10^{-9}$ | 1.568 | $2.40\times10^{-3}$ | $1.96\times10^{-4}$ | 1.599 |
| Variance | $100N_{F_i}$ | 61.57 | $1.233\times10^{-16}$ | 0.0505 | $3.1\times10^{-10}$ | $5.11\times10^{-8}$ | 0.0147 |

while keeping the same *Var* for each cluster, followed by 2000 independent two-level identifications in order to examine the impact of noise on the identified model parameters. It is important to bear in mind that, as explained further below after relationship (65), necessary constraints in the form of upper and lower bounds are imposed on each parameter within the identification program to ensure the admissibility of the identified parameters. We also made sure that the model parameters returned at the end of optimization runs are not close to their respective bounds.

Table 3 collects the mean and variance of the identified model parameters following 2000 identification runs for each cluster. Comparing the results of both clusters, one can see that by increasing the variance of the superposed noise, the variance of the identified parameters increases as well. Moreover, the mean values of the identified parameters from noisy data are further deviated from the corresponding reference values in Table 1 as the variance of the superposed noise grows. This observation is intuitively sensible because the more significant the impact of error sources on the fatigue data, the less accurately the model parameters would be identified. A similar performance and conclusion will most likely be obtained with other DAM variants. From among practical solutions that can help to improve the accuracy of the identified parameters, one may further enrich the fatigue database by running further fatigue tests and/or try to lower the impact of error sources by, for example, avoiding the stress concentrations when cutting the specimens, avoiding the misalignments when placing the specimens in the machine, minimizing the fluctuations in the test conditions such as temperature, and so on.

Histograms of Fig. 2 are constructed from the set of logarithm of model parameters identified using the second cluster of noisy fatigue data with $Var = 100N_{F_i}$. The normal distribution fits along with the mean values are superposed on each histogram. It can be seen that the histograms of $\log\ \sigma_{l_0}$, $\log\ b_1$, $\log\ \zeta$, $\log\ \eta$, and $\log\ \theta$ are more or less symmetric with the mean values located very close to the corresponding reference values of Table 1. On the contrary, the histogram of $\log\ b_2$, not only is unsymmetrical, it looks nothing like a normal distribution. Proximity of the mean values of the symmetric histograms to the reference values signifies that further enrichment of the database (that is, more fatigue data) leads to more satisfactory results for the corresponding model parameters, whereas there is no guarantee that the enrichment of the fatigue data will improve the accuracy of the identified $b_2$. The immediate conclusion to be drawn is that $b_2$ is identified with the highest level of uncertainty compared with other parameters.

## 4 Discussion and Generalization

The significance of the principal differential equation (10), which constitutes the core of this contribution, is that it covers all four possible cases of $\gamma(t)$ that may arise in multiaxial proportional cyclic loadings. This equation, however, has to be recast in the appropriate form compatible with the fatigue criterion to be utilized. To exemplify this point, Appendices A and B are devoted to the proper adaptation of the key differential equation to Sines and Crossland criteria and Dang Van criterion, respectively. Adaptation of this equation to Dang Van criterion, as elaborated in Appendix B, is not as straightforward as it is for Sines and Crossland criteria. The adaptation to Dang Van criterion is inspired by the form we obtained for Sines and Crossland criteria. This generalization idea can be most likely extended to other forms of adaptation required for other multiaxial fatigue criteria.

For the sake of validating the proposed approach, we take as an example, the HCF part of Sines-$H_{(ii)}$ variant and solve it for the number of cycles to failure of a single-block loading.

$$N_F = \theta \frac{1-\delta_0^{\left(\frac{A_{II}-A^*_{Sns}}{\sigma_u-\sigma_{eq_M}}\right)^\zeta}}{\mu} \left(\frac{A_{II}}{1-3b_2\bar{\sigma}_H}\right)^{-\theta} \left(\frac{\sigma_u-\sigma_{eq_M}}{A_{II}-A^*_{Sns}}\right)^\zeta \tag{63}$$

In the above relationship, setting $\delta_0 = 0$ and $\zeta = 1$, it matches Chaboche's HCF-DAM extended to 3D loading in Ref. [21] (Note that the coefficient "3" appearing behind $b_2$ in the above

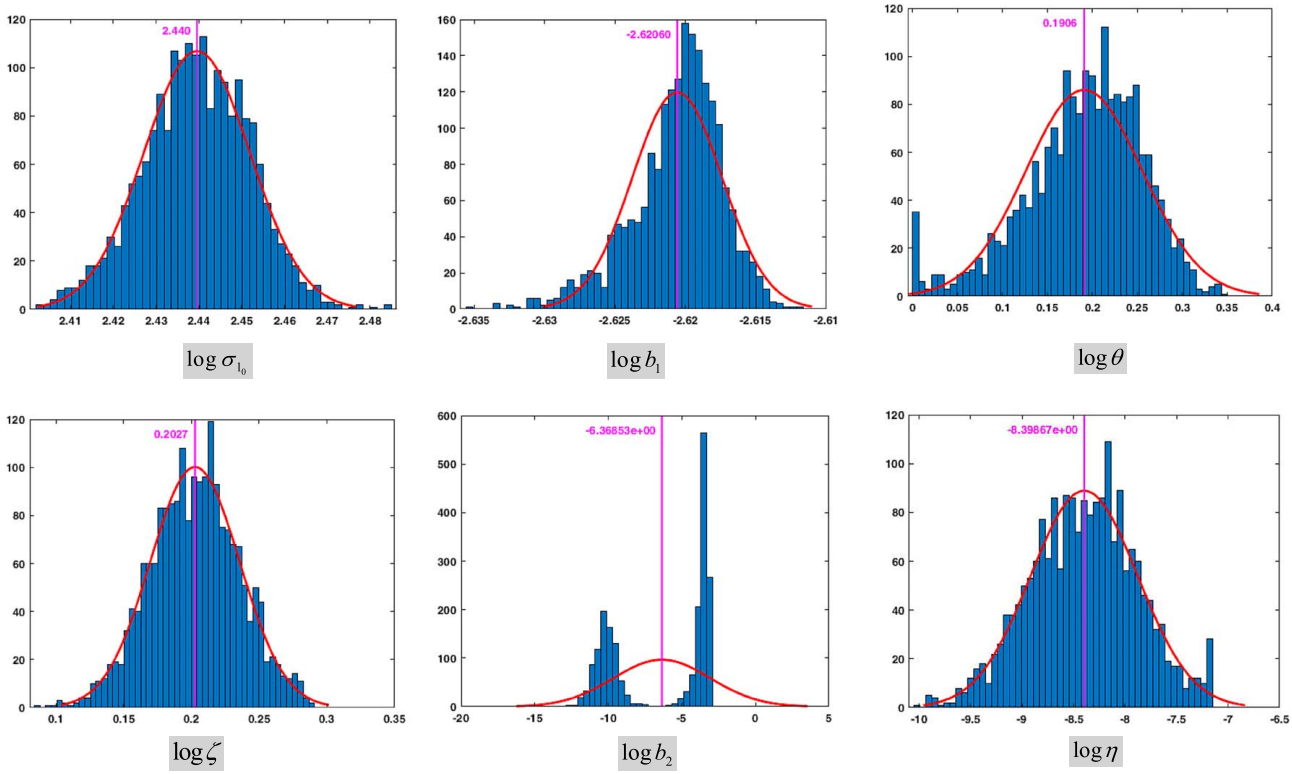


**Fig. 2 Histograms of the logarithm of model parameters from noisy fatigue data with Var = 100$N_F$ after 2000 times of superposition with noise followed by parameters identification.**

equation, is missing in the corresponding Eq. (25) in Ref. [21].). Except for parameters $\delta_0$ and $\zeta$, there is also a slight difference between the parameters of the above relationship and those of Eq. (25) in Ref. [21]. This is because we made use of $\mu = 4M_0(1+\theta)a$ as a new model parameter. It can be readily shown that the following relationship establishes the direct correspondence between both models. It also establishes the correspondence between Eq. (5) of Ref. [21] and Eq. (57) of this work.

$$\mu|_{\text{Sines}-H_{(\text{ii})}} = \eta|_{\text{Sines}-H_{(\text{i})}} = \beta(\beta+1)aM_0^{-\beta}|_{\text{Chaboche}} \tag{64}$$

Chaboche's fatigue damage model is thus retrieved as a specific case of our proposed (V)HCF-DAM to validate the derivation methodology of this contribution and to demonstrate its versatility.

Close examination of both variants of Sines-$H_{(\text{i})}$ and $-H_{(\text{ii})}$ reveals that they are basically identical. This is also the case of pair variants of Crossland and pair variants of Dang Van. This identity, however, is confined to these two forms of $H(D)$ and (V)HCF damage mechanisms. In case of choosing another form of $H(D)$ or the coupling of a different damage mechanism such as creep, this identity is no more valid.

Comparison of mathematical expressions of the above variants suggests that $M(\boldsymbol{\sigma})$ is independent of the form of $H(D)$ and this is true for other forms of $H(D)$ as well. We, therefore, conjecture that $M(\boldsymbol{\sigma})$ is exclusively a function of the adopted multiaxial fatigue criterion and once $M(\boldsymbol{\sigma})$ is determined for a given fatigue criterion with any $H(D)$, it can be stored and used directly with other forms of $H(D)$ and the same fatigue criterion.

On the question of model parameters identification, one needs to simplify the DAM variant of interest to uniaxial loading conditions in order to make it compatible with uniaxial fatigue tests, which are easily executable in the laboratory. Care should be taken that after reduction of 3D formulation to 1D, all model parameters appearing in 3D equations are preserved in the corresponding 1D equations as well. It can be seen that this is the case of Eqs. (25) and (57). This key feature applies to other DAM variants of this investigation, as well.

Regarding the model parameters, we opted for keeping $\lambda_0$, as a measure of initial damage in the specimens. In addition to that, the major advantage of introducing $\lambda_0$ is illustrated through relation (58). According to this relationship, the number of cycles to failure chosen by the user for defining $\sigma_{l_0}$, together with two other model parameters are interrelated. Moreover, the nonzero $\lambda_0$ controls the numerical value of $N_F$ as $\sigma_a \to \sigma_{l_0}(1-b_1\bar{\sigma})+\varepsilon$. Note that in case one sets $\lambda_0 = 0$, then $N_F$ grows unboundedly which is not physical, whereas with a proper nonzero $\lambda_0$, when $\sigma_a \to \sigma_{l_0}(1-b_1\bar{\sigma})+\varepsilon$, $N_F \to 10^7$ (or the subjective cycles to failure chosen by the user for setting $\sigma_{l_0}$).

For model parameters identification, we opted for building two appropriate nonnegative scalar functions whose global minimum correspond to the set of model parameters to identify. To define $OF_1$, we managed to eliminate $b_2$, which is subsequently identified in the second level using $OF_2$. We also noticed that if we re-identify $\eta$ along with $b_2$ in the second level of identification, the error of both $\eta$ and $b_2$ will be much lower; hence, a more robust identification scheme to noise. For both levels of identification, we used the GA toolbox of MATLAB as the global minimum search tool. The major characteristic feature of this optimization tool is that it is not gradient based and does not need the objective functions to be differentiable. Care has been taken to make sure that adjusting parameters of the GA tool had no impact whatsoever on the identified parameters. To make sure that the identified parameters are physically admissible, GA is set to fulfill the following upper and lower bounds for each parameter while searching for the global minimums.

$$\begin{array}{lll} 0.1\sigma_y < \sigma_{l_0} < 0.9\sigma_y & 0.1/\sigma_y < b_1 < 2/\sigma_y & 10^{-6}/\sigma_{ut} < b_2 < 2/\sigma_{ut} \\ 0.1 < \theta < 10 & 0.1 < \zeta < 10 & 10^{-30} < \eta < 10^{-3} \end{array} \tag{65}$$

It is worth noting that although $\sigma_y$ does not appear explicitly in the mathematical expression of different variants, it serves to define the constraints of $\sigma_{l_0}$ and $b_1$. This is the reason why $\sigma_y$ is given along with $\sigma_{ut}$ in Table 1 as material properties of SM490. In general, there is no rigorous method to determine the bounds of model parameters and this task strongly depends on the user's level of expertise. The bounds we suggest here are authors' recommendation based on several analyses of different alloys we tested and should not be taken as universally accepted ones. As a general rule, in case an identified parameter (almost) coincides either of its bounds, this specific bound ought to be modified properly before rerunning the identification in the presence of modified constraints.

The ad hoc identification procedure we expounded and implemented has efficiently identified the target model parameters from noisy fatigue data. The key feature of this procedure is that it can satisfactorily identify $\sigma_{l_0}$ from HCF tests with positive stress ratio. These are sole admissible HCF tests to perform on specimens with virtually zero resistance to buckling under compression. Although the entire identification scenario has been presented based on $R>0$ tests, it does not lose its generality and is equally applicable to HCF test data with any $-\infty<R<1$. One only needs to respect the guidelines given in Table 2 concerning the preparation of HCF test batches. Finally, it is understood that as a general rule, the richer the fatigue database, the more reliable the identified model parameters.

## 5 Summary and Concluding Remarks

To estimate the high cycle fatigue life of isotropic structures under multiaxial proportional loading, a formalism is laid out to derive the (V)HCF-DAM variants for metallic alloys subjected to multiaxial, multiblock, proportional, cyclic loadings. The backbone of this formalism is a differential equation with two degrees of freedom enabling the user to select or to fine-tune the DAM variant that satisfactorily captures the (V)HCF response of the alloy under study. To illustrate the performance of this formalism, six different variants are developed using three popular multiaxial fatigue criteria. Application of each fatigue criterion requires a kind of adaptation of the key differential equation, as has been the case for the fatigue criteria examined in this work. Chaboche's cumulative fatigue damage equation for 3D loading is recovered as a specific DAM variant of this article, thus corroborating the underlying assumptions and the key differential equation. Further concluding remarks are summarized as follows:

- For any multiaxial DAM, it is crucial that the model parameters appearing in the mathematical expression of multiaxial loading are preserved in the reduced form of uniaxial loading conditions. This is because the simplest fatigue tests to perform are uniaxial tests from which the model parameters will be identified. All DAM variants we have developed in this work fulfill this requirement.
- The model parameter corresponding to the initial damage in the specimens serves not only to generalize the formalism to metallic alloys other than ferrous and titanium alloys but also to control the cycles to failure of loading conditions close to loci of the points described by the adopted fatigue criterion.
- From among many scenarios tested for model parameters identification, the most efficient one consists of splitting the identification into two parts using two distinct nonnegative scalar objective functions. One of the parameters that are less successfully identified in the first level is re-identified in the second level, resulting in a far improved accuracy for this same parameter and another one that is identified in the second level.
- The proposed identification procedure not only is capable of identifying the model parameters efficiently but also identifies the material property $\sigma_{l_0}$ quite satisfactorily from tensile-tensile fatigue data (viz. $R>0$) that have additionally been superposed with white noise. These features underline the robustness and the efficacy of the proposed identification scheme.

## Nomenclature

$a$ = parameter of $\alpha$ function behind Macaulay brackets
$b$ = parameter of fatigue criteria
$D$ = damage variable
$Y$ = damage strain energy-releasing rate
$\mathbf{S}$ = deviatoric part of Cauchy stress tensor $\boldsymbol{\sigma}$
$A_{II}$ = octahedral shear stress amplitude
$D_0$ = initial damage of the specimen
$E_0$ = Young's modulus of the undamaged material
$J_{1/2}$ = 1st/2nd invariant of Cauchy stress tensor
$M_0$ = coefficient of function $M(\boldsymbol{\sigma})$
$N_{F_i}$ = number of cycles to failure in loading block $i$
$N'_{F_i}$ = noisy $N_{F_i}$ that is superposed with noise
$CFR$ = cycles to failure ratio
$H(D)$ = characteristic damage function
$M(\boldsymbol{\sigma})$ = stress function appearing in DAMs
$OF$ = nonnegative scalar objective function whose global minimum corresponds the best set of model parameters
$R=\sigma_m/\sigma_M$ = stress ratio
$R_p=\gamma_m/\gamma_M$ = proportionality ratio
$Var$ = variance

### Greek Letters

$\alpha$ = stress function used as an exponent in DAMs
$\gamma(t)$ = time coefficient of the proportional stress tensor
$\boldsymbol{\delta}_{ij}$ = Kronecker delta
$\delta=[1-(1-D)^{1+\theta}]^a$ = change of damage variable
$\zeta$ = parameter of fatigue DAMs
$\eta=4M_0a$ = change of DAM parameter
$\lambda=D^a$ = change of damage variable
$\lambda_0$ = a measure of the initial damage
$\theta$ = parameter of fatigue DAMs
$\mu=4M_0(1+\theta)a$ = change of DAM parameter
$\boldsymbol{\Sigma}(\boldsymbol{X})$ = time-independent stress tensor at point $\boldsymbol{X}$
$\sigma_u$ = ultimate tensile strength
$\bar{\sigma}$ = mean stress
$\sigma_{eq}$ = von Mises equivalent stress
$\boldsymbol{\sigma}(t, \boldsymbol{X})$ = time-varying stress tensor at point $\boldsymbol{X}$ and time $t$
$\sigma_y$ = yield stress
$\sigma_{l_0}$ = fatigue endurance limit
$\sigma_H=\sigma_{kk}/3$ = hydrostatic stress
$\tau_a$ = shear stress amplitude
$\upsilon$ = Poisson's ratio
$\phi(\boldsymbol{\sigma})$ = auxiliary stress function of Dang Van criterion
$\mathcal{N}(0, Var)$ = random number from the normal distribution with 0 mean and variance $Var$

### Subscripts or Superscripts

CL = related to Crossland criterion
DV = related to Dang Van criterion
M/m = maximum/minimum of the associated quantity
Sns = related to Sines criterion

**Acronyms and Abbreviations Widely Used in Text**

CDM = continuum damage mechanics
DAM = damage accumulation model
(V)HCF = (very) high cycle fatigue

## Appendix A: Adaptation of the Proposed DAM to Sines and Crossland Criteria

This appendix attempts to establish a relationship between the octahedral shear stress amplitude $A_{\text{II}}$ and maximum/minimum equivalent stresses ($\sigma_{\text{eq}_{\text{M/m}}}$) under proportional loading to adapt the key differential equation (10) to Sines and Crossland criteria. By definition, the time-varying proportional stress tensor $\boldsymbol{\sigma}$ at point $\boldsymbol{X}$ can be multiplicatively decomposed as $\boldsymbol{\sigma}(\boldsymbol{X}, t) = \gamma(t)\boldsymbol{\Sigma}(\boldsymbol{X})$. Let us consider two distinct time instants $t_1$, $t_2$ with the respective stress tensors ${}_1\boldsymbol{\sigma}$, ${}_2\boldsymbol{\sigma}$.

$$
{}_1\boldsymbol{\sigma} = \boldsymbol{\sigma}(\boldsymbol{X}, t_1) = \begin{bmatrix} \gamma_1\Sigma_{11} & \gamma_1\Sigma_{12} & \gamma_1\Sigma_{13} \\ \gamma_1\Sigma_{12} & \gamma_1\Sigma_{22} & \gamma_1\Sigma_{23} \\ \gamma_1\Sigma_{13} & \gamma_1\Sigma_{23} & \gamma_1\Sigma_{33} \end{bmatrix} = \gamma_1 \begin{bmatrix} \Sigma_{11} & \Sigma_{12} & \Sigma_{13} \\ \Sigma_{12} & \Sigma_{22} & \Sigma_{23} \\ \Sigma_{13} & \Sigma_{23} & \Sigma_{33} \end{bmatrix}
$$
$$
{}_2\boldsymbol{\sigma} = \boldsymbol{\sigma}(\boldsymbol{X}, t_2) = \begin{bmatrix} \gamma_2\Sigma_{11} & \gamma_2\Sigma_{12} & \gamma_2\Sigma_{13} \\ \gamma_2\Sigma_{12} & \gamma_2\Sigma_{22} & \gamma_2\Sigma_{23} \\ \gamma_2\Sigma_{13} & \gamma_2\Sigma_{23} & \gamma_2\Sigma_{33} \end{bmatrix} = \gamma_2 \begin{bmatrix} \Sigma_{11} & \Sigma_{12} & \Sigma_{13} \\ \Sigma_{12} & \Sigma_{22} & \Sigma_{23} \\ \Sigma_{13} & \Sigma_{23} & \Sigma_{33} \end{bmatrix} \tag{A1}
$$

Under cyclic loading, $\gamma(t)$ has a sinusoidal characteristic and can be described using its minimum and maximum values, $\gamma_{\text{m}}$ and $\gamma_{\text{M}}$, respectively. If the extrema of $\gamma(t)$ are denoted by $\gamma_1$ and $\gamma_2$, then $\gamma_{\text{m}} = \min\{\gamma_1, \gamma_2\}$ and $\gamma_{\text{M}} = \max\{\gamma_1, \gamma_2\}$. According to the diagrams of Fig. 1, the maximum and minimum values of von Mises equivalent stresses are obtained as follows:

$$
\begin{aligned}
\sigma_{\text{eq}_{\text{M}}} &= \max\{J_2(\boldsymbol{\sigma})\} = \max\{J_2(\gamma_{\text{m}}\boldsymbol{\Sigma}), J_2(\gamma_{\text{M}}\boldsymbol{\Sigma})\} \\
&= \max\{|\gamma_{\text{m}}|J_2(\boldsymbol{\Sigma}), |\gamma_{\text{M}}|J_2(\boldsymbol{\Sigma})\} = \max\{|\gamma_{\text{m}}|, |\gamma_{\text{M}}|\}J_2(\boldsymbol{\Sigma})
\end{aligned} \tag{A2}
$$

similarly,

$$
\begin{aligned}
\sigma_{\text{eq}_{\text{m}}} &= \min\{|\gamma_{\text{m}}|, |\gamma_{\text{M}}|\}J_2(\boldsymbol{\Sigma}) \\
J_2(\boldsymbol{\Sigma}) &= [(\Sigma_1 - \Sigma_2)^2 + (\Sigma_1 - \Sigma_3)^2 + (\Sigma_3 - \Sigma_2)^2]^{1/2}/\sqrt{2}
\end{aligned} \tag{A3}
$$

Here, $\Sigma_1$, $\Sigma_2$, and $\Sigma_3$ are principal stresses of $\boldsymbol{\Sigma}$. Evidently,

$$
\sigma_{\text{eq}_{\text{m}}}/\sigma_{\text{eq}_{\text{M}}} = \min\{|\gamma_{\text{m}}|, |\gamma_{\text{M}}|\}/\max\{|\gamma_{\text{m}}|, |\gamma_{\text{M}}|\} \tag{A4}
$$

A more convenient variable to use in the current formulations is the proportionality ratio, $R_{\text{p}} = \gamma_{\text{m}}/\gamma_{\text{M}}$. In reference with four cases illustrated in Fig. 1, it can be seen that

$$
\begin{aligned}
&\text{for case (a): } \sigma_{\text{eq}_{\text{m}}}/\sigma_{\text{eq}_{\text{M}}} = R_{\text{p}} \qquad \text{for case (b): } \sigma_{\text{eq}_{\text{m}}}/\sigma_{\text{eq}_{\text{M}}} = R_{\text{p}}^{-1} \\
&\text{for case (c): } \sigma_{\text{eq}_{\text{m}}}/\sigma_{\text{eq}_{\text{M}}} = -R_{\text{p}} \qquad \text{for case (d): } \sigma_{\text{eq}_{\text{m}}}/\sigma_{\text{eq}_{\text{M}}} = -R_{\text{p}}^{-1}
\end{aligned} \tag{A5}
$$

The above relations can be unified into a more general form of expression as follows:

$$
\sigma_{\text{eq}_{\text{m}}}/\sigma_{\text{eq}_{\text{M}}} = |R_{\text{p}}|^{\text{sign}(R_{\text{p}}+1)} \tag{A6}
$$

Using the definition of the octahedral shear stress amplitude for proportional loading, we obtain

$$
\begin{aligned}
A_{\text{II}} &= \frac{1}{2}\left|\max_t \gamma(t) - \min_{t_0} \gamma(t_0)\right| J_2(\boldsymbol{\Sigma}) \\
&= \frac{1}{2}(\max(|\gamma|) - \text{sign}(\gamma_{\text{m}}/\gamma_{\text{M}})\min(|\gamma|))J_2(\boldsymbol{\Sigma}) \\
&= \frac{1}{2}(\sigma_{\text{eq}_{\text{M}}} - \text{sign}(R_{\text{p}})\sigma_{\text{eq}_{\text{m}}})
\end{aligned} \tag{A7}
$$

Substitution from Eq. (A6) into (A7) leads to the following relationships;

$$
\begin{aligned}
\sigma_{\text{eq}_{\text{M}}} &= \frac{2A_{\text{II}}}{1 - \text{sign}(R_{\text{p}})|R_{\text{p}}|^{\text{sign}(R_{\text{p}}+1)}} \\
\sigma_{\text{eq}_{\text{m}}} &= \frac{2A_{\text{II}}|R_{\text{p}}|^{\text{sign}(R_{\text{p}}+1)}}{1 - \text{sign}(R_{\text{p}})|R_{\text{p}}|^{\text{sign}(R_{\text{p}}+1)}}
\end{aligned} \tag{A8}
$$

The expression inside brackets on the right-hand side of Eq. (10) can therefore be expressed as follows in terms of $A_{\text{II}}$.

$$
\sigma_{\text{eq}_{\text{M}}}^{\theta} - \text{sign}(R_{\text{p}})\sigma_{\text{eq}_{\text{m}}}^{\theta} = \frac{2^{\theta}A_{\text{II}}{}^{\theta}[1 - \text{sign}(R_{\text{p}})(|R_{\text{p}}|^{\text{sign}(R_{\text{p}}+1)})^{\theta}]}{[1 - \text{sign}(R_{\text{p}})|R_{\text{p}}|^{\text{sign}(R_{\text{p}}+1)}]^{\theta}} \tag{A9}
$$

In this way, the key differential Eq. (10) is recast into a compatible form with Sines and Crossland criteria as they are expressed as a function of $A_{\text{II}}$. In Appendix B, an attempt is made to express $\sigma_{\text{eq}_{\text{M}}}$ and $\sigma_{\text{eq}_{\text{m}}}$ in terms of the effective shear amplitude in order to make Eq. (10) compatible with Dang Van criterion.

## Appendix B: Adaptation of the Proposed Damage Accumulation Model to Dang Van Criterion

In analogy with Appendix A, here we try to find a relationship between $\sigma_{\text{eq}_{\text{M}}}$, $\sigma_{\text{eq}_{\text{m}}}$ and the shear stress amplitude, $\tau_{\text{a}}$, under multiaxial, proportional, cyclic loading. The general form of Dang Van criterion is expressed as follows [36,37]:

$$
\max_{\vec{n}} \max_t \left[\|\vec{\tau}(t) - \vec{\bar{\tau}}\| + \frac{3b\sigma_{\text{l}_0}}{2(1 - b\sigma_{\text{l}_0})}\sigma_{\text{H}}(t)\right] \le \frac{\sigma_{\text{l}_0}}{2(1 - b\sigma_{\text{l}_0})} \tag{B1}
$$

where $\vec{n}$ represents the normal to the plane that undergoes the maximum shear amplitude, $\vec{\tau}(t)$ is the shear vector that corresponds to $\boldsymbol{\sigma}\cdot\vec{n} - (\boldsymbol{\sigma}\cdot\vec{n}\cdot\vec{n})\vec{n}$, and $\vec{\bar{\tau}}$ represents the mean shear stress vector on this plane during the cyclic loading. The symbol $\|\|$ denotes the magnitude of the enclosed vector, and the hydrostatic stress $\sigma_{\text{H}}$ is related as follows to the first invariant of Cauchy stress tensor under proportional loading.

$$
\sigma_{\text{H}} = \frac{1}{3}J_1(\boldsymbol{\sigma}) = \frac{1}{3}\gamma(t)J_1(\boldsymbol{\Sigma}) = \frac{1}{3}\gamma(t)(\Sigma_1 + \Sigma_2 + \Sigma_3) \tag{B2}
$$

The plane of maximum shear stress remains unchanged under proportional loading, so once the plane of maximum shear stress is found, it does not change with time. Dang Van criterion (B1) can therefore be written in the following simpler form for a generic point $\boldsymbol{X}$ with the proportional stress state $\boldsymbol{\sigma}(\boldsymbol{X}, t) = \gamma(t)\boldsymbol{\Sigma}(\boldsymbol{X})$.

$$
\max_t \left[\|\vec{\tau}(t) - \vec{\bar{\tau}}\| + \frac{3b\sigma_{\text{l}_0}}{2(1 - b\sigma_{\text{l}_0})}\sigma_{\text{H}}(t)\right] \le \frac{\sigma_{\text{l}_0}}{2(1 - b\sigma_{\text{l}_0})} \tag{B3}
$$

The difference $\|\vec{\tau}(t) - \vec{\bar{\tau}}\|$ can be expanded as below under proportional loading conditions.

$$\begin{aligned}\|\vec{\tau}(t)-\vec{\bar{\tau}}\| &= \left|\tau(t)-\frac{\tau_{\mathrm{M}}+\tau_{\mathrm{m}}}{2}\right| \\ &= \left|\gamma(t)\frac{\max\{\Sigma_1,\Sigma_2,\Sigma_3\}-\min\{\Sigma_1,\Sigma_2,\Sigma_3\}}{2}-\frac{\gamma_{\mathrm{M}}+\gamma_{\mathrm{m}}}{2}\frac{\max\{\Sigma_1,\Sigma_2,\Sigma_3\}-\min\{\Sigma_1,\Sigma_2,\Sigma_3\}}{2}\right| \\ &= \left|\gamma(t)-\frac{\gamma_{\mathrm{M}}+\gamma_{\mathrm{m}}}{2}\right|\frac{\max\{\Sigma_1,\Sigma_2,\Sigma_3\}-\min\{\Sigma_1,\Sigma_2,\Sigma_3\}}{2}\end{aligned} \tag{B4}$$

Accordingly,

$$\begin{aligned}&\underset{t}{\mathrm{Max}}\left[\|\vec{\tau}(t)-\vec{\bar{\tau}}\|+\frac{3b\sigma_{\mathrm{l}_0}}{2(1-b\sigma_{\mathrm{l}_0})}\sigma_{\mathrm{H}}(t)\right] \\ &= \underset{t}{\mathrm{Max}}\left[\left|\gamma(t)-\frac{\gamma_{\mathrm{M}}+\gamma_{\mathrm{m}}}{2}\right|\frac{\max\{\Sigma_1,\Sigma_2,\Sigma_3\}-\min\{\Sigma_1,\Sigma_2,\Sigma_3\}}{2}+\frac{b\sigma_{\mathrm{l}_0}}{2(1-b\sigma_{\mathrm{l}_0})}\gamma(t)(\Sigma_1+\Sigma_2+\Sigma_3)\right] \\ &= \frac{\max\{\Sigma_1,\Sigma_2,\Sigma_3\}-\min\{\Sigma_1,\Sigma_2,\Sigma_3\}}{2}\underset{t}{\mathrm{Max}}\left[\left|\gamma(t)-\frac{\gamma_{\mathrm{M}}+\gamma_{\mathrm{m}}}{2}\right|\right]+\frac{b\sigma_{\mathrm{l}_0}}{2(1-b\sigma_{\mathrm{l}_0})}(\Sigma_1+\Sigma_2+\Sigma_3)\underset{t}{\mathrm{Max}}\,\gamma(t)\end{aligned} \tag{B5}$$

Evidently, the time-dependent, sinusoidal functions $|\gamma(t)-(\gamma_{\mathrm{M}}+\gamma_{\mathrm{m}})/2|$ and $\gamma(t)$ reach their maxima simultaneously since the frequency of their maxima is the same. This means that the maximum of the sum of both terms inside the square brackets of the second line in Eq. (B5) corresponds to the sum of the maximum of each term, hence the last relationship of Eq. (B5). Moreover,

$$\underset{t}{\mathrm{Max}}\left[\left|\gamma(t)-\frac{\gamma_{\mathrm{M}}+\gamma_{\mathrm{m}}}{2}\right|\right]=\frac{\gamma_{\mathrm{M}}-\gamma_{\mathrm{m}}}{2},\qquad \underset{t}{\mathrm{Max}}\,\gamma(t)=\gamma_{\mathrm{M}} \tag{B6}$$

Substituting Eq. (B6) into Eq. (B5) results in the following simpler form of representation of Dang Van fatigue criterion specialized to proportional loading.

$$\frac{\max\{\Sigma_1,\Sigma_2,\Sigma_3\}-\min\{\Sigma_1,\Sigma_2,\Sigma_3\}}{2}\frac{\gamma_{\mathrm{M}}-\gamma_{\mathrm{m}}}{2}+\frac{b\sigma_{\mathrm{l}_0}}{2(1-b\sigma_{\mathrm{l}_0})}(\Sigma_1+\Sigma_2+\Sigma_3)\gamma_{\mathrm{M}}\le\frac{\sigma_{\mathrm{l}_0}}{2(1-b\sigma_{\mathrm{l}_0})} \tag{B7}$$

The above representation of Dang Van criterion can be rendered more practical by introducing the extrema of oscillating principal stresses.

$$\begin{aligned}&\left|\frac{\max\{\sigma_{1_{\mathrm{M}}},\sigma_{2_{\mathrm{M}}},\sigma_{3_{\mathrm{M}}}\}-\min\{\sigma_{1_{\mathrm{M}}},\sigma_{2_{\mathrm{M}}},\sigma_{3_{\mathrm{M}}}\}}{2}-\frac{\max\{\sigma_{1_{\mathrm{m}}},\sigma_{2_{\mathrm{m}}},\sigma_{3_{\mathrm{m}}}\}-\min\{\sigma_{1_{\mathrm{m}}},\sigma_{2_{\mathrm{m}}},\sigma_{3_{\mathrm{m}}}\}}{2}\right| \\ &+\frac{b\sigma_{\mathrm{l}_0}}{1-b\sigma_{\mathrm{l}_0}}(\sigma_{1_{\mathrm{M}}}+\sigma_{2_{\mathrm{M}}}+\sigma_{3_{\mathrm{M}}})\le\frac{\sigma_{\mathrm{l}_0}}{1-b\sigma_{\mathrm{l}_0}}\end{aligned} \tag{B8}$$

To express the shear stress amplitude in terms of maximum/minimum shear stresses,

$$\begin{aligned}\tau_{\mathrm{a}} &= \underset{t}{\mathrm{Max}}\,\|\vec{\tau}(t)-\vec{\bar{\tau}}\|=\frac{\gamma_{\mathrm{M}}-\gamma_{\mathrm{m}}}{2}\frac{\max\{\Sigma_1,\Sigma_2,\Sigma_3\}-\min\{\Sigma_1,\Sigma_2,\Sigma_3\}}{2} \\ &= \frac{\max\{|\gamma_{\mathrm{m}}|,|\gamma_{\mathrm{M}}|\}-\mathrm{sign}(R_{\mathrm{p}})\min\{|\gamma_{\mathrm{m}}|,|\gamma_{\mathrm{M}}|\}}{2}\times\frac{\max\{\Sigma_1,\Sigma_2,\Sigma_3\}-\min\{\Sigma_1,\Sigma_2,\Sigma_3\}}{2} \\ &= \frac{1}{2}(\tau_{\mathrm{eq}_{\mathrm{M}}}-\mathrm{sign}(R_{\mathrm{p}})\tau_{\mathrm{eq}_{\mathrm{m}}})\end{aligned} \tag{B9}$$

Hence, the safe region described by Dang Van criterion specialized to proportional loading is simplified to the following form:

$$\tau_{\mathrm{a}}-\frac{\sigma_{1_0}(1-3b\sigma_{\mathrm{H_M}})}{2(1-b\sigma_{1_0})}<0 \tag{B10}$$

Although we managed to find a relationship between $\tau_{\mathrm{a}}$, $\tau_{\mathrm{eq}_{\mathrm{M}}}$, and $\tau_{\mathrm{eq}_{\mathrm{m}}}$, the load variables appearing in the key damage evolution differential equation (10) are the maximum and minimum Von Mises equivalent stresses $\sigma_{\mathrm{eq}_{\mathrm{M}}}$ and $\sigma_{\mathrm{eq}_{\mathrm{m}}}$. Seemingly, an explicit relationship between $\tau_{\mathrm{a}}$, $\sigma_{\mathrm{eq}_{\mathrm{M}}}$, and $\sigma_{\mathrm{eq}_{\mathrm{m}}}$ is impossible. For this reason, use is made of the following idea, inspired by relationship (A9).

Closer examination of relation (A9) and the ensuing damage evolution equations suggests that the expression next to ${A_{\mathrm{II}}}^{\theta}$ in Eq. (A9) does not appear in the final damage evolution equations. This implies that if the complicated coefficient multiplied by ${A_{\mathrm{II}}}^{\theta}$ is replaced with a general function of the stress tensor, say $\psi(\boldsymbol{\sigma})$, and Eq. (A9) is rewritten as

$$\sigma_{\mathrm{eq}_{\mathrm{M}}}^{\theta}-\mathrm{sign}(R_{\mathrm{p}})\sigma_{\mathrm{eq}_{\mathrm{m}}}^{\theta}={A_{\mathrm{II}}}^{\theta}\psi(\boldsymbol{\sigma}) \tag{B11}$$

then by following a similar procedure and without having to know the exact form of $\psi(\boldsymbol{\sigma})$, the same damage evolution equations are obtained. By analogy, we postulate that a relationship similar to Eq. (B11) exists between $\tau_{\mathrm{a}}$, $\sigma_{\mathrm{eq}_{\mathrm{M}}}$ and $\sigma_{\mathrm{eq}_{\mathrm{m}}}$ using some unknown auxiliary function $\phi(\boldsymbol{\sigma})$ such that

$$\sigma_{\mathrm{eq}_{\mathrm{M}}}^{\theta}-\mathrm{sign}(R_{\mathrm{p}})\sigma_{\mathrm{eq}_{\mathrm{m}}}^{\theta}=\tau_{\mathrm{a}}^{\theta}\phi(\boldsymbol{\sigma}) \tag{B12}$$

Assuming the validity of such a relationship, the governing differential Eq. (13) can be expressed as follows in $\tau_a$.

$$\frac{(1-D)^{\theta}\mathrm{d}D}{H(D)} = \frac{M(\boldsymbol{\sigma})}{\theta}{\tau_a}^{\theta}\phi(\boldsymbol{\sigma})\mathrm{d}N \tag{B13}$$

In this way, the governing differential equation of our proposed damage evolution model is adapted for employing Dang Van criterion.

## References


[1] Wöhler, A., 1870, *Über die Festigkeitsversuche mit Eisen und Stahl*, Ernst & Korn, Berlin.
[2] Basquin, O. H., 1910, "The Exponential Law of Endurance Tests," Proc. ASTM, pp. 625–630.
[3] Palmgren, A., 1924, "Die Lebensdauer von Kugellagern," Z. VDI, **58**(14), pp. 339–341.
[4] Miner, M. A., 1945, "Cumulative Damage in Fatigue," ASME J. Appl. Mech., **12**(3), pp. 159–164.
[5] Marco, S. M., and Starkey, W. L., 1954, "A Concept of Fatigue Damage," Trans. ASME, **76**(4), pp. 627–632.
[6] Palin-Luc, T. (1996). Fatigue Multiaxiale d'une fonte GS Sous Sollicitations Combinées D'amplitude Variable. ENSAM de Paris. https://www.theses.fr/1996ENAM0029.
[7] Fatemi, A., and Yang, L., 1998, "Cumulative Fatigue Damage and Life Prediction Theories: a Survey of the State of the Art for Homogeneous Materials," Int. J. Fatigue, **20**(1), pp. 9–34.
[8] Chaboche, J. L., 1988, "Continuum Damage Mechanics: Part I—General Concepts," ASME J. Appl. Mech., **55**(1), pp. 59–64.
[9] Chaboche, J. L., 1988, "Continuum Damage Mechanics: Part II—Damage Growth, Crack Initiation, and Crack Growth," ASME J. Appl. Mech., **55**(1), pp. 65–72.
[10] Lemaitre, J., 1996, *A Course on Damage Mechanics*, Springer Berlin Heidelberg, Berlin, Heidelberg.
[11] Lemaitre, J., and Desmorat, R., 2005, *Engineering Damage Mechanics*, Springer-Verlag, Berlin, Heidelberg.
[12] Murakami, S., 2012, *Continuum Damage Mechanics*, Springer Netherlands, Dordrecht.
[13] Rabotnov, Y., 1969, *Creep Problems in Structural Members*, North-Holland Pub. Co., Amsterdam.
[14] Rabotnov, Y. N., Leckie, F. A., and Prager, W., 1970, "Creep Problems in Structural Members," ASME J. Appl. Mech., **37**(1), p. 249.
[15] Kachanov, L. M., 1986, *Introduction to Continuum Damage Mechanics*, Springer Netherlands, Dordrecht.
[16] Rodin, G. J., 2000, "Continuum Damage Mechanics and Creep Life Analysis," ASME J. Appl. Mech., **67**(1), pp. 193–196.
[17] Robinson, D. N., and Binienda, W. K., 2005, "A Representation of Anisotropic Creep Damage in Fiber Reinforced Composites," ASME J. Appl. Mech., **72**(4), pp. 484–492.
[18] Chaboche, J. L., 1974, "Une loi différentielle d'endommagement de fatigue avec cumulation non linéaire," Rev. Française Mécanique, **50**(51), pp. 71–82.
[19] Chaboche, J. L., and Lesne, P. M., 1988, "A non-Linear Continuous Fatigue Damage Model," Fatigue Fract. Eng. Mater. Struct., **11**(1), pp. 1–17.
[20] Chaudonneret, M., 1993, "A Simple and Efficient Multiaxial Fatigue Damage Model for Engineering Applications of Macro-Crack Initiation," ASME J. Eng. Mater. Technol., **115**(4), pp. 373–379.
[21] Marmi, A. K., Habraken, A. M., and Duchene, L., 2009, "Multiaxial Fatigue Damage Modelling at Macro Scale of Ti–6Al–4V Alloy," Int. J. Fatigue, **31**(11–12), pp. 2031–2040.
[22] Xiao, Y.-C., Li, S., and Gao, Z., 1998, "A Continuum Damage Mechanics Model for High Cycle Fatigue," Int. J. Fatigue, **20**(7), pp. 503–508.
[23] Do Van, V. N., Lee, C.-H., and Chang, K.-H., 2015, "High Cycle Fatigue Analysis in Presence of Residual Stresses by Using a Continuum Damage Mechanics Model," Int. J. Fatigue, **70**, pp. 51–62.
[24] Lee, C.-H., Chang, K.-H., and Van Do, V. N., 2016, "Modeling the High Cycle Fatigue Behavior of T-Joint Fillet Welds Considering Weld-Induced Residual Stresses Based on Continuum Damage Mechanics," Eng. Struct., **125**, pp. 205–216.
[25] Gerber, W. Z., 1874, "Calculation of the Allowable Stresses in Iron Structures," Z. Bayer Arch. Ing. Ver., **6**(6), pp. 101–110.
[26] Goodman, J., 1899, *Mechanics Applied to Engineering*, Longman, Green and Co, London.
[27] Haigh, B. P., 1917, "Experiments on the Fatigue of Brasses," J. Inst. Met., **18**, pp. 55–86.
[28] Soderberg, C. R., 1939, "Factor of Safety and Working Stress," Trans. ASME, **52**(2), pp. 13–28.
[29] Papadopoulos, I. V., Davoli, P., Gorla, C., Filippini, M., and Bernasconi, A., 1997, "A Comparative Study of Multiaxial High-Cycle Fatigue Criteria for Metals," Int. J. Fatigue, **19**(3), pp. 219–235.
[30] Papadopoulos, I. V., 1998, "Critical Plane Approaches in High-Cycle Fatigue: on the Definition of the Amplitude and Mean Value of the Shear Stress Acting on the Critical Plane," Fatigue Fract. Eng. Mater. Struct., **21**(3), pp. 269–285.
[31] Carpinteri, A., and Spagnoli, A., 2001, "Multiaxial High-Cycle Fatigue Criterion for Hard Metals," Int. J. Fatigue, **23**(2), pp. 135–145.
[32] Papuga, J., 2011, "A Survey on Evaluating the Fatigue Limit Under Multiaxial Loading," Int. J. Fatigue, **33**(2), pp. 153–165.
[33] Mamiya, E. N., Castro, F. C., and Araújo, J. A., 2014, "Recent Developments on Multiaxial Fatigue: The Contribution of the University of Brasília," Theor. Appl. Fract. Mech., **73**, pp. 48–59.
[34] Sines G., 1959, "Behavior of Metals Under Complex Static and Alternating Stresses," *Metal Fatigue*, G. Sines, J. L. Waisman, and T. J. Dolan, eds., pp. 145–169, McGraw-Hill, New York.
[35] Crossland, B., 1956, "Effect of Large Hydrostatic Pressures on the Torsional Fatigue Strength of an Alloy Steel," Proceedings of the International Conference on Fatigue of Metals, Institution of Mechanical Engineers, London, pp. 138–149.
[36] Dang Van K., Griveau B., and Message O., 1989, "On a New Multiaxial Fatigue Limit Criterion: Theory and Application," *ICBMFF2, Biaxial and Multiaxial Fatigue*, EFG-3, M. W. Brown, and K. J. Miller, eds., pp. 479–496, Mechanical Engineering Publications, London.
[37] Dang-Van K., 1993, "Macro-Micro Approach in High-Cycle Multiaxial Fatigue," *Advances in Multiaxial Fatigue*, p. 120, ASTM International, 100 Barr Harbor Drive, PO Box C700, West Conshohocken, PA 19428-2959.
[38] Carpinteri, A., De Freitas, M., and Spagnoli, A., 2003, "Biaxial/Multiaxial Fatigue and Fracture," 6th International Conference on Biaxial/Multiaxial Fatigue and Fracture, Elsevier.
[39] Lemaitre, J., 1984, "How to Use Damage Mechanics," Nucl. Eng. Des., **80**(2), pp. 233–245.
[40] Lemaitre, J., and Dufailly, J., 1987, "Damage Measurements," Eng. Fract. Mech., **28**(5–6), pp. 643–661.
[41] Lemaitre, J., 1986, "Local Approach of Fracture," Eng. Fract. Mech., **25**(5–6), pp. 523–537.
[42] Kintzel, O., Khan, S., and Mosler, J., 2010, "A Novel Isotropic Quasi-Brittle Damage Model Applied to LCF Analyses of Al2024," Int. J. Fatigue, **32**(12), pp. 1948–1959.
[43] Patil, N., Mahadevan, P., and Chatterjee, A., 2008, "A Constructive Empirical Theory for Metal Fatigue Under Block Cyclic Loading," Proc. R. Soc. A Math. Phys. Eng. Sci., **464**(2093), pp. 1161–1179.
[44] Chaboche J.-L., 2013, "Cumulative Damage," *Fatigue of Materials and Structures*, pp. 47–110, John Wiley & Sons, Inc., Hoboken, NJ.
[45] Dattoma, V., Giancane, S., Nobile, R., and Panella, F. W., 2006, "Fatigue Life Prediction Under Variable Loading Based on a New non-Linear Continuum Damage Mechanics Model," Int. J. Fatigue, **28**(2), pp. 89–95.
[46] Kaminski, M., Kanouté, P., Gallerneau, F., Chaboche, J. L., and Kruch, S., 2005, "Lifetime Predictions Under Complex Loading for a Car Application," Fatigue Design Conf. on CETIM, Senlis.
[47] Lemaitre, J., and Chaboche, J.-L., 1990, *Mechanics of Solid Materials*, Cambridge University Press, Cambridge.
[48] Sabirov, I., Enikeev, N. A., Murashkin, M. Y., and Valiev, R. Z., 2015, *Multifunctional Properties of Bulk Nanostructured Metallic Materials*, Springer Cham, New York, pp. 27–100.